Defence Research and
Development Canada

Recherche et développement
pour la défense Canada

DEFENCE **R&D** DÉFENSE

Ship Signatures in RADARSAT-1 ScanSAR Narrow B Imagery
Analysis with AISLive Data

Paris W. Vachon, Ryan A. English and John Wolfe

Defence R&D Canada – Ottawa

Canadá

Ship Signatures in RADARSAT-1 ScanSAR Narrow B Imagery

Analysis with AISLive Data

Paris W. Vachon
DRDC Ottawa

Ryan A. English
DRDC Ottawa

John Wolfe
DRDC Ottawa

Defence R&D Canada – Ottawa

Principal Author

Original signed by Paris W. Vachon

Paris W. Vachon

Defence Scientist

Approved by

Original signed by Gary W. Geling

Gary W. Geling

Head, Radar Applications and Space Technologies

Approved for release by

Original signed by Cam Boulet

Cam Boulet

Chair, Document Review Panel

Abstract

RADARSAT-1 ScanSAR Narrow B (SCNB) mode imagery at 50 m (nominal) spatial resolution of high density shipping regions were acquired along with contemporaneous Automatic Identification System (AIS) data via an AISLive snapshot service. Within the images are 1805 signatures of isolated ships ranging from 40 m to 350 m in length, for which AIS data, including ship identification, size, and velocity, are available.

The AIS data were verified through an authoritative ship database, which identified errors in the static AIS data. Dynamic errors were also characterized since pairs of location observations were available. The mean error between the AIS-predicted ship position and the ship signature position (124 m) is smaller than the average ship length in the overall data set (147 m).

The data were used to model the radar cross section (RCS) of ships in SCNB data as a simple geometric function of the ship length. The variability about the normalized RCS, a consequence of ship type, local incidence angle, ship aspect angle, and sea state, could not be described by a single probability density function, but a Log-Normal distribution was appropriate for certain ship length ranges. Ship RCS variability observed in the SCNB data is consistent with that observed previously in Fine mode data, but there is an overall scaling differing between the SCNB and Fine mode data sets.

This work demonstrates that the fusion of RADARSAT image signatures of ships with AIS data is straightforward and provides unprecedented insight to observed ship signatures. However, the AIS data, at least the static fields, should be routinely verified prior to fusion with other sources of ship information.

Résumé

Des images ScanSAR à faisceau étroit B (SCNB) de RADARSAT-1, d'une résolution spatiale au sol de 50 m (nominale) des régions maritimes à haute densité de trafic ont été acquises en même temps que des données du Système d'identification automatique (SIA) du service d'instantanés AISLive. Les images contiennent 1805 signatures de navires isolés, de 40 à 350 mètres de longueur, pour lesquelles des données SIA, incluant l'identification, la taille, et la vitesse, sont disponibles.

Les données SIA ont été contrôlées par rapport à une base de données officielle de navires, ce qui a permis de détecter des erreurs dans les données statiques SIA. Les erreurs dynamiques ont également été caractérisées grâce aux paires d'observations d'emplacement disponibles. L'erreur moyenne entre la position d'un navire prédit par le SIA et la position de la signature du navire (124 mètres) est plus petite que la longueur moyenne des navires de l'ensemble des données (147 mètres).

Les données ont été utilisées pour modéliser la section efficace radar (RCS) des navires dans les données SCNB en tant que fonction géométrique simple de la longueur des navires. La variabilité des RCS normalisées, une conséquence du type de navire, de l'angle d'incidence local, de l'angle de l'aspect du navire et l'état de la mer, ne pouvait pas être décrite par une simple fonction de densité de probabilité, toutefois une distribution log normale convenait pour certaines plages de longueurs de navire. La variabilité de la section efficace des navires qui a été observée dans les données SCNB correspond à avec celle qui a été observée auparavant dans les données en mode fin, mais il y a une différence d'échelle entre les données SCNB et les données en mode fin.

L'étude démontre que la fusion des signatures d'images RADARSAT de navires et des données SIA est simple et fournit une possibilité inouïe quant à l'observation des signatures de navires. Toutefois, les données SIA, du moins les champs statiques, devraient être automatiquement vérifiées avant de fusionner avec d'autres sources de renseignements sur les navires.

Executive summary

Ship Signatures in RADARSAT-1 ScanSAR Narrow B Imagery: Analysis with AISLive Data

Vachon, P.W., English, R.A., Wolfe, J.; DRDC Ottawa TM 2007-052; Defence R&D Canada – Ottawa; March 2007.

Introduction

This document considers data analysis from the reprise of an experiment that was conducted in 2005 in which DRDC Ottawa obtained contemporaneous RADARSAT-1 Fine mode data at 8 m (nominal) spatial resolution and AISLive snapshot service Automatic Identification System (AIS) data for ship validation. The objective of the 2005 experiment was to develop a database of validated ship signatures in RADARSAT-1 imagery for automatic target recognition training. The data also proved to be valuable for ship radar cross section (RCS) modelling. The reprise focussed on RADARSAT-1 ScanSAR Narrow B (SCNB) mode data at 50 m (nominal) spatial resolution, a mode that is similar to the RADARSAT-2 mode that will be used by the Polar Epsilon Project for near-real time surveillance of the ocean approaches to Canada. The AISLive snapshot service was modified to provide snapshot pairs that bracketed the predicted RADARSAT-1 acquisition times. The acquisition times were predicted using the Commercial Satellite Imagery Acquisition Planning System (CSIAPS).

Results

The experiment resulted in a data set comprised of 23 SCNB images of high density shipping regions including Strait of Dover, Strait of Gibraltar, and Busan Strait that were matched to the AISLive snapshot data. Within the images were 1805 signatures of isolated ships ranging from 40 m to 350 m in length, and for which AIS data, including ship identification, size, and velocity, are available.

It was found that CSIAPS was able to predict the RADARSAT-1 acquisition time to within a few seconds, provided CSIAPS was run roughly one week in advance of the pass time. This pass time planning and data acquisition strategy allows more reliable matching of AIS data to observed ship signatures in the RADARSAT-1 data, and permits examination of certain error types in dynamic AIS data.

It was found that the AISLive data contains inherent errors relative to an authoritative ship database. These errors might reflect the error rates in AIS data in general. Ship identification errors were relatively rare but do occur. Ship length was in error for nearly 10% of the ships considered. Errors in dynamic data also occur but are more difficult to quantify. Use of bracketing AISLive snapshot data sets reduced error that could be associated with single AISLive snapshot dead reckoning. The mean error between the AIS-predicted ship position and the ship signature position (124 m) is smaller than the average ship length in the overall data set (147 m).

The total RCS of the SCNB ship data was modelled as a simple geometric function of the ship length. The variability about the normalized RCS, a consequence of ship type, local incidence angle, ship aspect angle, and sea state, to name a few, could not be described by a single probability density function, but a Log-Normal distribution was appropriate for certain ship length ranges.

The variability of the normalized SCNB ship RCS data is the same as the variability of the normalized Fine mode ship RCS data that were acquired in 2005. However, the two data sets differ by the normalization function that was used in each case, which amounts to a few dB over the available range of ship lengths. Presumably this difference can be ascribed to the RCS being slightly dependent upon the resolution at which the data were acquired.

Significance

This data set and the associated analysis demonstrates that the fusion of RADARSAT image signatures of ships with AIS data is straightforward, even in high density shipping regions, although interpolation and azimuth shifting operations are essential to obtaining reliable results. It is recommended that AIS data, at least the static fields, be routinely verified through an authoritative ship database prior to fusion with other sources of ship information. Analysis of the dynamic fields, by comparing track positions with the reported velocity for example, can reveal AIS implementation errors that could impact the fusion of AIS data with SAR image signatures.

Ship RCS variability observed in the SCNB data is consistent with that observed previously in Fine mode data, but there is an overall scaling differing between the SCNB and Fine mode data sets. A single probability density function that describes the variability in the data sets could not be found. Nevertheless, it is recommended that the SCNB ship RCS model function and the Log-Normal distribution be used for RADARSAT-2 SCNB data to reduce false alarms in operational software. Note that image product dynamic range saturation could lead to underestimation of the ship RCS.

Future plans

RADARSAT data is acquired at a single polarization (i.e., HH). An Envisat ASAR data set with various polarizations has also been acquired and is currently being analyzed. This data set will be valuable in understanding and modelling the polarization dependence of ship RCS and ship target contrast. The ability to model the probability density function of the ship RCS could be improved by considering more complex model functions.

Sommaire

Ship Signatures in RADARSAT-1 ScanSAR Narrow B Imagery: Analysis with AISLive Data

Vachon, P.W., English, R.A., Wolfe, J.; DRDC Ottawa TM 2007-052; R & D pour la défense Canada – Ottawa; mars 2007.

Introduction

Le présent document analyse les données recueillies lors de la reprise d'une expérience déjà menée en 2005 par RDDC Ottawa, qui avait acquis des données en mode fin RADARSAT-1 à une résolution au sol de 8 m (nominale) et des données contemporaines du Système d'identification automatique (SIA) du service d'instantanés AISLive pour la validation des navires. L'objectif de l'expérience de 2005 était de mettre sur pied une base de données de signatures de navires validées par l'imagerie RADARSAT-1 pour les exercices de reconnaissance automatique de cibles. Les données ont aussi prouvées leur valeur quant à la modélisation de la section efficace radar (RCS). La reprise de l'expérience était axée sur les données ScanSAR à faisceau étroit B (SCNB) de RADARSAT-1. d'une résolution spatiale au sol de 50 m (nominale), un mode semblable au mode RADARSAT-2 qui sera utilisé par le projet Polar Epsilon pour la surveillance en temps quasi réel des approches océaniques du Canada. Le service d'instantanés AISLive a été modifié pour fournir des paires d'instantanés qui couvrent les temps d'acquisition prévus de RADARSAT-1. Les heures d'acquisition ont été prédits par le Système de planification d'acquisition d'images de satellites commerciaux (CSIAPS).

Résultats

L'expérience a fourni un ensemble de données comportant 23 images SCNB des régions maritimes à haute densité de trafic, incluant le Pas de Calais, le détroit de Gibraltar et le détroit de Corée qui ont été comparées aux données AISLive. Les images contiennent 1805 signatures de navires isolés, de 40 à 350 mètres de longueur, pour lesquelles des données SIA, incluant l'identification, la taille, et la vitesse, sont disponibles.

Le programme CSIAPS a été capable de prédire l'heure d'acquisition RADARSAT-1 en quelques secondes, sous réserve qu'il ait été exécuté environ une semaine avant le passage du satellite. La planification de l'heure de passage et la stratégie d'acquisition de données a permis des jumelages plus précis de données SIA avec les signatures de navires observées dans les données RADARSAT-1, ainsi que l'examen de certains types d'erreurs dans les données dynamiques SIA.

On a constaté que les données AISLive contiennent des erreurs inhérentes par rapport à une base de données officielle de navires. Ces erreurs peuvent refléter les taux d'erreurs dans les données SIA en général. Les erreurs d'identification de navires ont été relativement rares, mais elles se sont produites. Il y a une erreur de la longueur de 10 % des navires repérés. Des erreurs dans les données dynamiques ont également été révélées, mais il a toutefois été plus difficile de les quantifier. L'utilisation d'ensembles de données d'instantanés qui couvrent les temps

d'acquisition Radarsat a réduit les erreurs qui auraient pu être associées à des instantanés AISLive pris à l'estime. L'erreur moyenne entre la position d'un navire prédite par le SIA et la position de la signature du navire (124 mètres) est plus petite que la longueur moyenne des navires de l'ensemble des données (147 mètres).

Les données ont été utilisées pour modéliser la section efficace radar des navires dans les données SCNB en tant que fonction géométrique simple de la longueur des navires. La variabilité des RCS normalisées, une conséquence du type de navire, de l'angle d'incidence local, de l'angle d'aspect du navire et de l'état de la mer, ne pouvait pas être décrite par une simple fonction de densité de probabilité, mais une distribution log normale convenait pour certaines plages de longueurs de navire.

La variabilité des données RCS normalisées SCNB est la même que celle des données RCS normalisées en mode fin qui ont été acquises en 2005. Cependant, les deux ensembles de données diffèrent pour la fonction de normalisation qui a été utilisée dans chaque cas, différence qui atteint quelques dB pour la plage disponible de longueurs de navire. Il est probable que cette différence soit attribuable au fait que la RCS dépend quelque peu de la résolution d'acquisition des données.

Importance

Cet ensemble de données et l'analyse qui y est associée démontrent que la fusion de la signature de navires d'images RADARSAT avec les données SIA est simple, même dans les régions maritimes à haute densité de trafic, mais des opérations d'interpolation et de modification d'azimuts sont essentielles pour obtenir des résultats précis. Il est recommandé que les données SIA, du moins les champs statiques, soient automatiquement vérifiées avant de fusionner avec d'autres sources de renseignements sur les navires. L'analyse des champs dynamiques, par la comparaison de positions de trajectoires avec la vitesse rapportée par exemple, peut révéler des erreurs SIA qui pourraient avoir un impact sur la fusion des données SIA avec les signatures d'images SAR.

La variabilité de la section efficace radar des navires dans les données SCNB correspond à celle qui a été observée auparavant dans les données en mode fin, mais il y a une différence d'échelle entre les données SCNB et les données en mode fin. Une simple fonction de densité de probabilité, qui décrit la variabilité de l'ensemble de données, n'a pu être trouvée. Il est quand même recommandé que la fonction de modèle de la section efficace de navire SCNB et la distribution log normale soient utilisées pour les données SCNB de RADARSAT-2 pour réduire les fausses alertes dans le logiciel opérationnel. Il faut noter que la saturation de la plage dynamique des images pourrait mener à une sous-estimation de la section efficace radar des navires.

Perspectives

Les données RADARSAT sont recueillies à une seule polarisation. (c.-à-d. HH). Un ensemble de données ASAR ENVISAT avec polarisations multiples a également été recueilli et est en cours d'analyse. Cet ensemble de données sera d'une grande valeur dans la compréhension et la modélisation de la dépendance à l'égard de la polarisation de la section efficace radar de navire et

du contraste navire-cible. Les capacités de modélisation de la fonction de densité de probabilité de la section efficace radar de navire pourrait être améliorées par des fonctions de modélisation plus complexes.

This page intentionally left blank.

Table of contents

List of figures

List of tables

Acknowledgements

1.   Introduction

In 2005, Defence R&D Canada – Ottawa (DRDC Ottawa) combined Automatic Identification System (AIS) data with ship signatures in RADARSAT-1 (R-1) synthetic aperture radar (SAR) imagery in order to develop a database for automatic target recognition (ATR) training [8]. The initial activity focussed on the highest resolution R-1 data available, i.e., Fine mode at 8 m (nominal) resolution, for proof of concept. As a source of AIS data DRDC Ottawa contacted AISLive, a commercial provider, who were able to provide an AIS snapshot service that was matched to the nominal satellite pass times. Three high-density shipping regions were chosen that are covered by AISLive: the Straits of Dover, the Straits of Gibraltar, and the Busan Strait. This trial eventually yielded 399 Fine mode ship signatures that were used to develop models for ship radar cross section (RCS) [8] and its probability density function (PDF) [10].

Operational maritime surveillance typically trades-off spatial resolution in order to obtain wider area coverage. Furthermore, the operational near-real time ship detection capability that will be implemented by Project Polar Epsilon using RADARSAT-2 imagery will use a mode that is similar to the R-1 ScanSAR Narrow B (SCNB) mode at 50 m (nominal) resolution. Therefore, a reprise of the 2005 trial was proposed, but using SCNB (composed of single beams W2, S5, and S6). The objective was to obtain a new data set to evaluate the applicability of the Fine mode results to SCNB. Similarly, new ship RCS models could help to improve performance prediction for future C-band SAR missions.

In addition to position, AIS data provides several identifiers about each ship – its name, its call-sign, its International Maritime Organization (IMO) registration number, its Maritime Mobile Service Identity (MMSI) number – as well as information about its state, such as heading and speed. Access to the unique identifiers for the ships allowed further data-mining by cross-referencing these IDs with the Internet Ships Register (ISR) Database (http://www.ships-register.com), maintained by Lloyd's Register – Fairplay, allowing information about vessel specification in the AIS reports to be verified in the ISR Database.

Predicting the AIS-reported ship position at the satellite-pass time is crucial to matching the AIS-reported information with the correct target signature in the satellite image. High frequency AIS data would be very useful for this exercise; however, it was not a practical solution given the limited resources available. In the 2005 R-1 Fine beam AIS analysis [8], a single AIS-snapshot was used to predict the ship positions. For most cases, the results were very good provided the vessel did not turn or accelerate in the time span between the AIS acquisition and the SAR pass.

To improve the available validation data at the satellite-pass time, two AIS-snapshots were collected for the 2006 dataset, one prior to the R-1 start acquisition time and one after the R-1 stop acquisition time. Furthermore, the large coverage area provided by SCNB significantly increases the number of imaged targets in each scene, as compared to Fine mode coverage, requiring a corresponding increase in the AIS collection boundaries.

This document is arranged as follows: Section 2 describes the acquired SCNB data set and how the R-1 pass times were predicted relative to the AISLive matching service; Section 3 describes the processing of the acquired SAR imagery; Section 4 discusses the use of the AISLive data to provide an AIS-predicted ship signature position in the SAR imagery; Section 5 summarizes an

error analysis of the AISLive data; Section 6 contains examples of ship signatures in SCNB imagery that are matched to available AIS data; Section 7 discusses an analysis of the ship RCS in terms of an overall model function and a PDF to describe the RCS variability; and finally, Section 8 contains a comparison of the 2005 Fine mode data and the 2006 SCNB data. The conclusions of this work are presented in Section 9.

2.   Data Acquisition

The SCNB and AISLive data acquired during this trial are summarized as follows:

- 36 R-1 SCNB mode acquisitions were ordered;

- 2 R-1 acquisitions were abandoned (i.e., lost to higher priority acquisitions in a different mode);

- 3 R-1 acquisitions were lost due to payload anomaly;

- 2 R-1 data sets have Doppler processing problems that we have not so far been able to resolve;

- 1 AISLive acquisition was lost; and

- 5 AISLive acquisitions have time code errors.

This activity yielded a set of 23 R-1 SCNB image with contemporaneous AISLive data sets for analysis.

2.1   Acquisition Planning Using SPA and CSIAPS

The RADARSAT Swath Planner Application (SPA) is a software tool provided by RADARSAT International (RSI) and is the de facto standard for R-1 acquisition planning. SPA uses a nominal orbit and conservative swath coverage to provide the acquisition analysis. A more advanced planning application, the Commercial Satellite Imagery Acquisition Planning System (CSIAPS), has been developed by DRDC Ottawa with MDA as the development contractor [5]. CSIAPS uses actual orbit data and orbit propagation software to provide the acquisition analysis.

For planning purposes, estimates of image acquisition times were generated using both SPA and CSIAPS, with the CSIAPS centre time being used to refine the acquisition time estimate as the date of acquisition approached. The acquisition time estimates for the ordered R-1 imagery was used to estimate the desired AISLive acquisition times; AIS snapshots were requested for both 90 seconds before and 90 seconds after the CSIAPS centre time for each image. The planned and actual acquisition times for the data collected are given in Table 1.

Comparing the SPA and the CSIAPS centre times with the Raw Data centre times for the 23 cases considered, we found that the SPA-predicted pass time was different by 144.3±3.0 seconds, on average, while the CSIAPS-predicted pass time was different by -5.8±18.4 seconds, on average. However, for the 3 initial cases on June 1, 4, and 6, the R-1 orbit data were not properly updated in CSIAPS, so the time differences are larger in those cases. For the 20 cases in which the orbit data were correctly updated, the CSIAPS-predicted centre time was different from the Raw Data centre time by 0.8±6.1 seconds, on average. Given the requirement to provide accurate pass times to obtain the contemporaneous AIS data, we recommend use of CSIAPS, in particular to be run within a week of the expected pass time, if possible, so that the orbit data are up to date, to provide accurate predicted R-1 pass times.

Table 1. Planned and actual acquisition times in Univesal Time Coordinated (UTC) for R-1 SCNB imagery and AIS data. The first 8 are Busan; the next 9 are Gibraltar; and the final 6 are Dover.

	Date	SPA	CSIAPS	Actual	Δt_{SPA} (s)	Δt_{CSIAPS} (s)	AISLive Time 1	AISLive Time 2
1	1-Jun-06	21:24:47	21:21:48	21:22:27	140.0	-38.9	21:20:19	21:23:19
2	4-Jun-06	09:21:09	09:17:54	09:18:49	139.5	-55.9	9:16:55	9:19:54
3	8-Jun-06	21:20:38	21:18:23	21:18:18	140.0	5.0	21:17:23	21:20:23
4	25-Jun-06	21:24:47	21:22:34	21:22:25	142.0	9.0	21:21:34	21:24:34
5	28-Jun-06	09:21:09	09:18:41	09:18:46	143.0	-5.0	9:17:42	9:20:42
6	15-Jul-06	09:25:16	09:22:48	09:22:50	146.0	-2.5	9:21:49	9:24:49
7	22-Jul-06	09:21:09	09:18:38	09:18:45	144.0	-7.0	9:17:39	9:20:38
8	26-Jul-06	21:20:38	21:18:18	21:18:14	144.0	4.0	21:17:20	21:20:20
1	6-Jun-06	18:27:08	18:23:53	18:24:47	141.0	-53.8	18:22:53	18:25:53
2	30-Jun-06	18:27:08	18:24:41	18:24:44	144.0	-3.0	18:23:41	18:26:41
3	5-Jul-06	06:26:09	06:23:47	06:23:43	146.0	4.5	6:22:48	6:25:47
4	7-Jul-06	18:22:59	18:20:29	18:20:32	147.0	-3.5	18:19:30	18:22:29
5	12-Jul-06	06:21:59	06:19:33	06:19:33	146.0	-0.5	6:18:32	6:21:32
6	24-Jul-06	18:27:08	18:24:40	18:24:34	154.0	6.0	18:23:41	18:26:40
7	29-Jul-06	06:26:09	06:23:46	06:23:45	144.0	1.0	6:22:46	6:25:46
8	31-Jul-06	18:22:59	18:20:28	18:20:35	144.0	-6.5	18:19:00	18:21:59
9	5-Aug-06	06:21:59	06:19:34	06:19:35	144.0	-1.0	6:18:34	6:21:34
1	5-Jul-06	17:45:18	17:42:47	17:42:52	146.0	-5.0	17:41:48	17:44:47
2	9-Jul-06	06:05:01	06:02:44	06:02:34	147.0	10.5	6:01:44	6:04:44
3	16-Jul-06	06:00:49	05:58:32	05:58:24	145.0	7.5	5:57:33	6:00:32
4	2-Aug-06	06:05:01	06:02:44	06:02:37	144.0	6.5	6:01:44	6:04:45
5	5-Aug-06	17:41:08	17:38:33	17:38:44	144.0	-11.0	17:37:37	17:40:33
6	9-Aug-06	06:00:49	05:58:30	05:58:24	145.0	6.5	5:57:31	6:00:32

Each data set consists of one image and two AIS snapshots, one acquired prior to the pass time and one acquired after the pass time, collected nominally 3 minutes apart. The vessel data recorded in each snapshot, however, have a time latency of between 0 and 180 seconds. This means that despite the image being nominally bracketed by the two snapshots, there will be vessels with both AIS broadcasts preceding the image acquisition.

Figure 1 shows the data latencies for a representative case from Dover on 9-Aug-2006. The image centre time is at 05:58:24, 6 seconds earlier than predicted with CSIAPS, and 2 minutes 5 seconds earlier than predicted by SPA. From the post-image snapshot, 721 AIS reports are time-stamped after the image centre time and 70 (8.8%) are listed as reporting before. Only 7 of these are underway with a speed greater than 0.5 knots, two others are underway with a speed less than 0.5 knots, with the remainder moored, anchored or reporting zero speed. AIS specifications only require stationary vessels to report their position every 6 minutes, with the frequency of reports increasing as the speed of the vessel increases, which should account for the bulk of the latencies. Since the AIS broadcasts are line-of-sight over Very High Frequency (VHF) radio frequencies, communication errors may account for the high latency in the 7 vessels at speed.
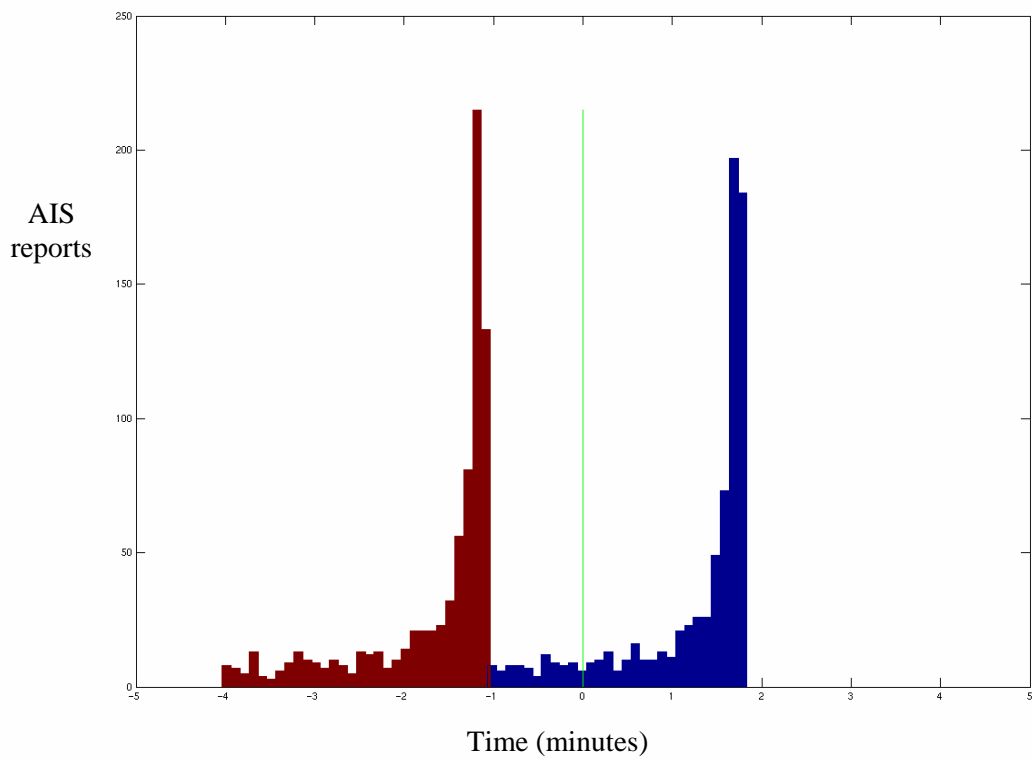
Figure 1. Histogram of latencies from AIS broadcast times by the originating vessels to the AISLive snapshot acquistion time for the Dover, 9-Aug-2006 collection. The pre-image snapshot (red) and post-image snapshot (blue) are shown relative to the image centre time (green line), which occurred 6 seconds earlier than predicted by CSIAPS.

3.   SAR Data Processing

The initial plan was to obtain 8-bit, radiometrically-calibrated image products from the Canadian Data Processing Facility (CDPF) based upon a "mixed" output look-up table (LUT). However, we immediately realized that, for these products, the ship signatures of interest would be saturated within the available 8-bit dynamic range. We tried to compensate for this by having the data re-processed using a point target output LUT. These new products, though more successful, still had significant target saturation problems.

Unfortunately, DRDC Ottawa did not have a supported R-1 ScanSAR processor available in house. As such, the burst mode module was procured for the available Advanced Precision Processor (APP) [11] that is in routine use. This processor optionally provides floating point output products, which are not radiometrically saturated and do not require use of an output LUT. The calibration of the APP floating point product was verified against that of the CDPF products and was found to be very close.

The overall processing strategy for this project was to obtain raw data product from the CDPF, and to base our analysis on floating point image products produced using APP. It should be noted that RCS measurements based upon saturated 8-bit image products would, in general, be underestimated relative to the floating point products that we used in this work.

Aside from the ship signature position, the main analysis step was estimating of the ship signature total RCS. A VUSAR-like algorithm [13], in which an image chip is analyzed, and a clutter estimate based upon the four corners of the image chip, was used. Ship RCS estimates from the VUSAR algorithm have previously been compared with results from other exploitation tools [7].

4.   AIS Data Processing

The goal of using AIS data is to establish a correspondence between information about a ship in the database and its SAR signature in the R-1 imagery. Vessel motion will cause a separation between the signature and the AIS-reported positions, both along the track of a ship due to time differences between the AIS-report and the image acquisition, and in the azimuthal direction of the image due to a Doppler shift of the ship signature. Further differences may arise due to issues with image registration, Global Position System (GPS) time stamps, AISLive snapshot database time stamps, non-linear ship motion, ship accelerations, on-board GPS antenna location, and other sources of errors.

By processing the data to correct for the largest position shifts, most AIS-reported positions for vessels within the confines of the image can be uniquely matched to a signature in the imagery, even using a single AIS report [8]. The introduction of the second AIS report allows us to avoid further sources of error by interpolating the position of the ship between the snapshots, where possible, rather than relying upon vessel-provided heading and speed. The data processing methodology consists of the following:

- Project the vessel position from the bracketing AIS-*reported* ship positions to correspond to the satellite pass times to produce the set of AIS-*projected* positions;

- Azimuth-shift the AIS-projected positions to the set of AIS-*predicted* positions to account for the Doppler frequency shift of moving targets;

- Locate the ship signature given the AIS-predicted position and perform target analysis if a valid signature is found;

- Perform filtering operations such as land masking; and

- Gather statistics and carry out data analysis, as warranted.

4.1   AIS-Projected Position

Each AISLive snapshot provides four characteristic parameters that serve to constrain the geometry of the vessel's track over time, namely: time t, position $\vec{X}$, Heading H, and Speed over Ground (SoG) S. Ideally, one would use Course over Ground (CoG) rather than Heading, but AISLive only provides AIS CoG in the Heading field when AIS Heading is not available; the two can be distinguished by noting that AIS CoG is formatted to one decimal place, while AIS Heading is integer. The presence of AIS CoG is found in 1741 cases out of the 18,857 AIS entries (9.2%), 587 of them with AIS SoG above 0.5 knots.

The simplest approach to projecting the vessel position from an AISLive snapshot is to use dead-reckoning (DR), whereby the new position is shifted in the direction H by a distance of $S(t-T)$, where T is the image acquisition time. So long as the AIS-reported Heading and Speed are consistent with the actual position changes of the vessel, DR provides a reasonably good estimate for allowing the pairing of AIS and signature positions [8]. For a small, but

significant, number of vessels, inconsistencies have been observed to the extent that a more refined method is required to resolve the uncertainties about these targets.

Data from the two AISLive snapshots, which we index by $j \in \{i, f\}$ to indicate the source being either the *initial* (ideally pre-image) or *final* (ideally post-image) snapshot, is used to develop an interpolation method for projecting the vessel position. The majority of entries in each snapshot can be matched to an entry in the other for that vessel. When such vessels are underway and manoeuvring, we can use the combined data to improve the approximation of the vessel position at the image acquisition time. Primarily, we consider the circumstances when the image acquisition occurs between the AIS broadcasts captured by each AIS snapshot, but the approach does provide useful information to improve results when both AIS broadcasts occur before the image acquisition or both occur after.

Using the two snapshot datasets independently, DR will give approximate positions to serve as initial conditions for an azimuthal shift correction, but unless the vessel's actual CoG and SoG remain constant and the AIS fields are error free, these estimations may differ considerably. In particular, if the vessel has effected a manoeuvre, neither set of conditions may be close to the conditions required to implement a correct azimuthal shift. Instead, we propose the following methodology.

Initially, our assumption was that vessels only engage in a single manoeuvre between the AIS snapshots. This assumption was quickly abandoned as it was unable to adapt to cases where the Heading remained constant, $H_{f^\cdot} = H_i$, but differed from CoG calculated as the bearing of the vector between the two points, $C_0 = \arg(\vec{X}_f - \vec{X}_i)$, relative to true north. We note that, in general, the Great Circle path between points is not of constant course, yet constant course is the natural method of travel for maritime vessels. This issue has been resolved through the use of the Mercator Projection [1], in which straight lines are indeed paths of constant course, called loxodromes or rhumb lines, over the Earth's surface.

To convert geodetic coordinates $\vec{X}_j = (\lambda_j, \psi_j)$, where λ is the longitude and ψ the latitude, into Mercator coordinates, we use [12]:

$$
\begin{aligned}
x_j &= R_E \ \text{rad}\left(\lambda_j - \lambda_0\right), \\
y_j &= \frac{1}{2} R_E \ln\left(\frac{1 + \sin\left(\psi_j\right)}{1 - \sin\left(\psi_j\right)}\right),
\end{aligned}
\tag{1}
$$

where λ_0 is any reference meridian, so we choose $\lambda_0 = \lambda_i$ whereby $x_i = 0$.

Normalizing the distance scale to the x-direction, the y scaling becomes:

$$\Sigma = \frac{R_E(\psi_f - \psi_i)}{\rho \cos(C_0)} \qquad (2)$$

where $\rho = \sqrt{(x_f - x_i)^2 + (y_f - y_i)^2}$ is the rhumb line distance between the two points.

In an ideal, error-free situation, the vessel will travel a distance of $D = \frac{1}{\Sigma}\left(\frac{S_f + S_i}{2}\right)(t_f - t_i)$. For a non-manoeuvring vessel, we expect $D = \rho$. However, rarely do the AIS SoG and Heading exactly produce this result. We therefore independently calculate estimates for CoG and SoG.

We assume that the positions and times are precise, whereby the vector, $\vec{D}_0$, connecting the two points is characterized by angle C_0 and length $\rho = S_0 \Delta t$, C_0 and S_0 being the zeroth order approximations to course and speed, respectively.

The estimated path of the vessel is then approximated by three segments. There are two cases to be considered, depending on whether the path must cross $\vec{D}_0$ or not in order to satisfy the initial AIS CoG conditions, as shown in Figure 2. In the case where the path need not cross, C_0 lies between C_i and C_f. The path is therefore constructed of a circular arc whose endpoint tangents have angles C_i at $\vec{X}_i$ and C_0 at the other, a straight line with bearing C_0, and a final circular arc subtending from C_0 to C_f. A single degree of freedom remains that determines the radii of the arcs, the offset, δ of the path from the vector, and subsequently the total path length. In the case where the path crosses the vector, the straight line component has a calculated bearing of $C_1 = C_0 + \omega$, where ω is the angular offset that parameterizes the remaining degree of freedom, the arc radii, and the total path length.

The path length, $D_{total}(\delta, \omega)$, is calculated by summing the three components, scaled to correct for the Mercator Projection, and compared to the maximum distance the vessel might have traveled by using $D_{max} = \max_j (S_j)(t_f - t_i)$. If $D_{total}(0,0) > D_{max}$, then the reported speeds cannot produce the required track between GPS positions. This is resolved by assuming an actual speed of $S_t = D_{total}(0,0)/(t_f - t_i)$. Otherwise, we can solve $D_{total}(\delta, 0) = D_{max}$ or $D_{total}(0, \omega) = D_{max}$, depending on which case we have. Another alternative is to equate D_{total} to $D_{avg} = (S_i + S_f)(t_f - t_i)/2$. Since there are a wide range of possible SoG variations for manoeuvring vessels to exhibit, and there is currently insufficient rationale to prefer one constraint over the other, we have chosen to implement the constraint $D_{total} = D_{test}$, where $D_{test} = (D_{max} + D_{avg})/2$.

A choice of constraint other than D_{avg} will require that $S(t)$ vary quadratically with time, but with three constraints – two points and one distance – the quadratic parameters can be solved for. With these calculations in hand, the path can then be parameterized according to time, $t \in [t_i, t_f]$, along with corresponding CoG and SoG values, $C(t)$ and $S(t)$, respectively. Should the image acquisition time, t_{acq}, be outside this interval, DR is implemented using the calculated endpoint

values, $\left(C(t_j), S(t_j) \right)$ with $j = \begin{cases} i, & t_{acq} < t_i, \\ f, & t_{acq} > t_f. \end{cases}$

(a)   (b)
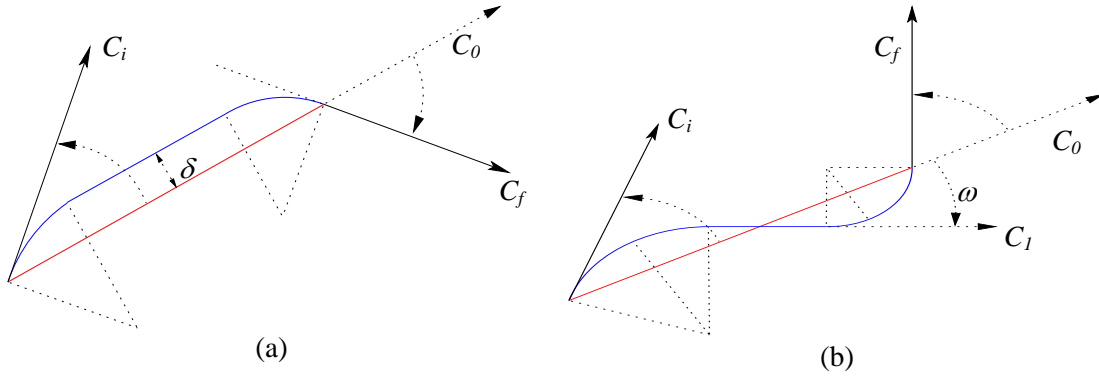
Figure 2. The two cases for interpolation. The $\vec{D}_0$ vector is in red, the estimated path $\vec{D}_{total}$ is in blue. Initial, final, zero-th approximation, and first approximation courses are C_i, C_f, C_0, and C_1, respectively. The path length is a function of: a) the offset δ for the non-crossing case; and b) the angular offset ω for the crossing case.

4.2   AIS-Predicted Position

The AIS-*projected* positions are azimuth shifted to AIS-*predicted* positions to account for the Doppler frequency shift of moving targets based upon the AIS-reported velocity and the satellite geometry. The effective shift in azimuth (Δ_{az} in meters) is:

$$\Delta_{az} = \frac{R_s V_r}{V_{sc}} \tag{3}$$

where R_s is the spacecraft to target slant range in meters, V_r is the radial velocity of the ship in m/s, and V_{sc} is the spacecraft velocity in m/s. V_r is defined as:

$$V_r = \chi \times \mathrm{S}_{proj} \times \cos(\phi)\cos(\theta_{inc})\tag{4}$$

where S_{proj} is the projected ship speed over ground in m/s, ϕ is the difference between the platform look direction and the projected course over ground (C_{proj}) expressed in radians, and θ_{inc} is the target incidence angle expressed in radians. For APP-generated descending mode products $\chi = -1.0$; APP-generated ascending mode products $\chi = +1.0$. Then $\phi = \mathrm{rad}\left[90° - \chi\left(C_{proj} - \mathrm{LH}\right)\right]$, where LH is the azimuth line heading expressed in degrees[1].

An example of the interpolation and azimuth shift of AIS-reported positions is provided in Figure 3. This R-1 SCNB image chip acquired over Gibraltar on 5 July 2006 illustrates the DR of the bracketing AIS-snapshots (blue and red lines), the interpolation to AIS-projected position (intersection of green and yellow lines), and the azimuth-shift operation (green line) to the AIS-predicted position (the + sign). The position information indicates the ship was turning during acquisition and illustrates the capability of the interpolation step. Figure 4 is a R-1 SCNB image chip acquired over Dover on 16 July 2006 and illustrates accurate position predictions for numerous AIS-reported positions. Figure 5 presents a more challenging case.

---

[1] These azimuth shift equations apply to APP-generated image products which are oriented north-up, west-left. Special attention (i.e., modifications) would be required to properly interpret CDPF products, particularly ScanSAR image products, since they are oriented in acquisition coordinates and use a different definition for LH.
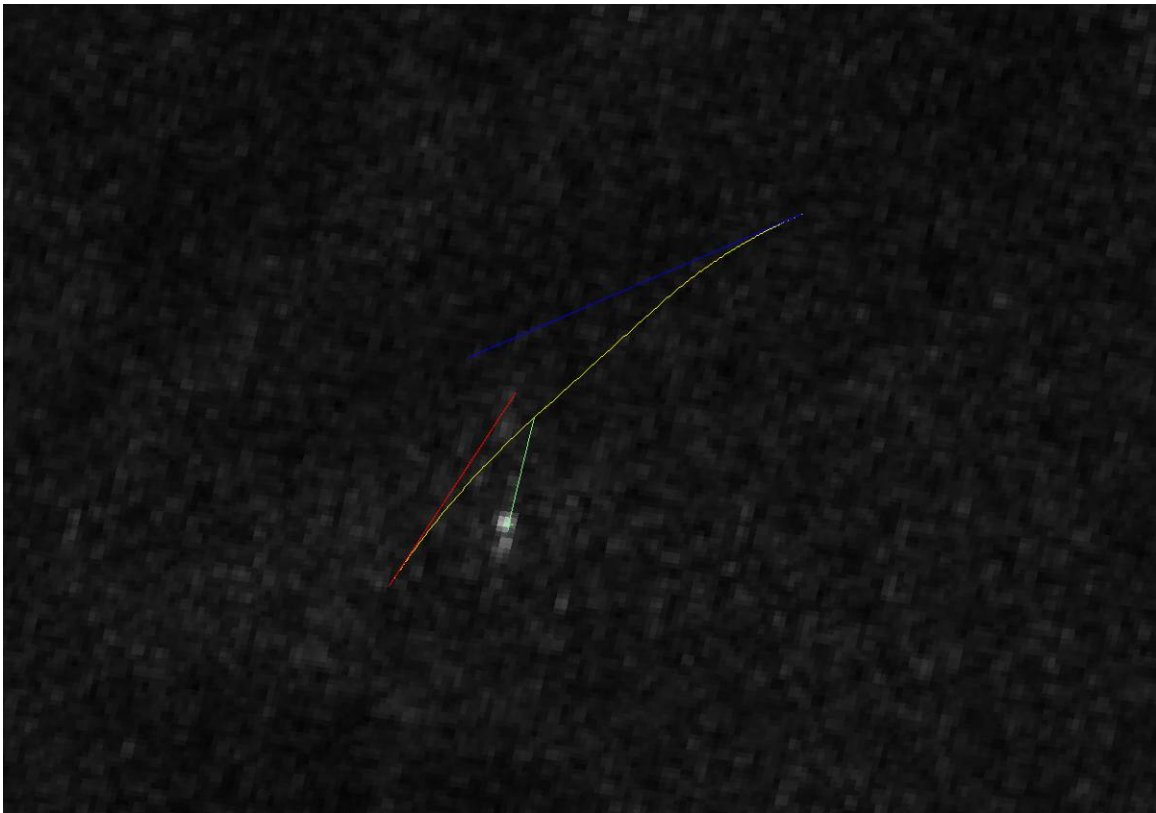
Figure 3. This R-1 SCNB image chip acquired over Gibraltar on 5 July 2006 illustrates the dead-reckoning of the bracketing AIS-snapshots (blue and red lines), the interpolation to AIS-projected position (intersection of green and yellow lines), and the azimuth-shift operation (green line) to the AIS-predicted position (+ sign).
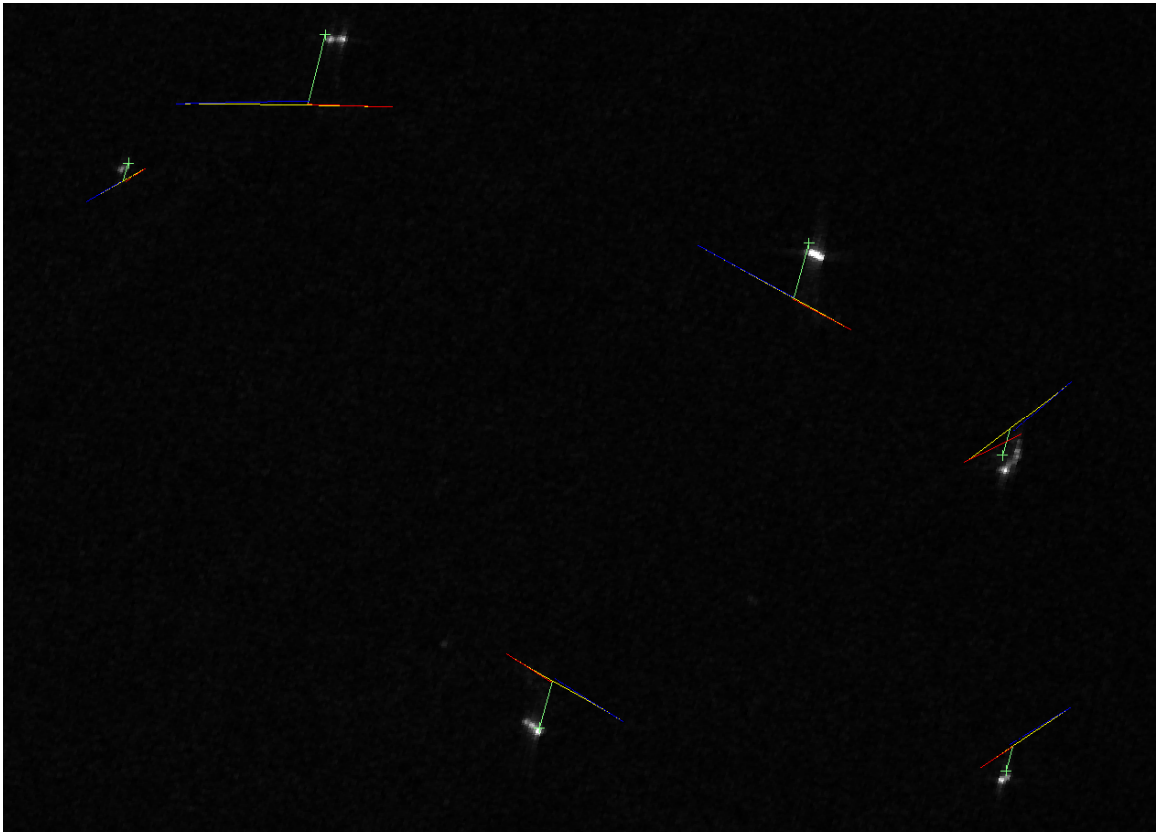
Figure 4. This R-1 SCNB image chip acquired over Dover on 16 July 2006 illustrates the dead-reckoning of the bracketing AIS-snapshots (blue and red lines), the interpolation to AIS-projected positions (yellow lines), and the azimuth-shift operation (green lines) to the AIS-predicted positions (+ signs).

(a)
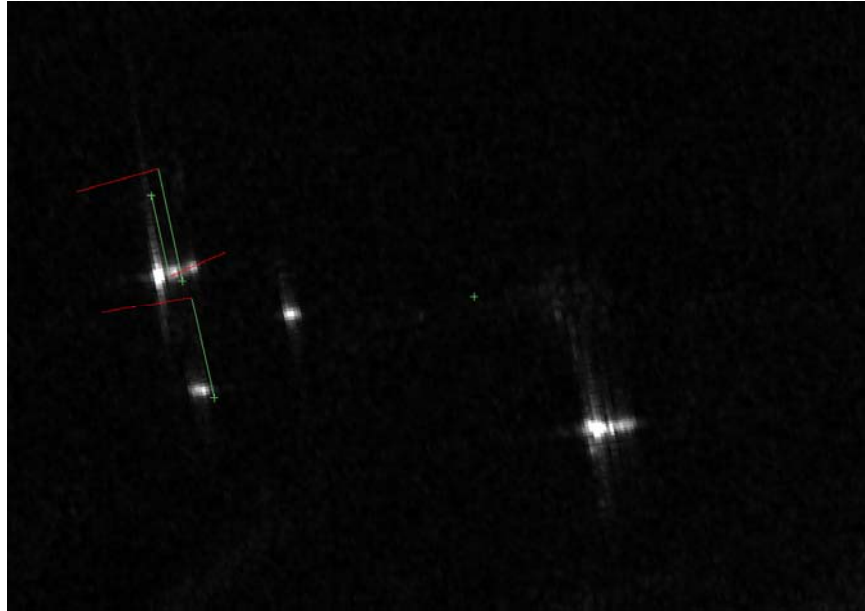
(b)
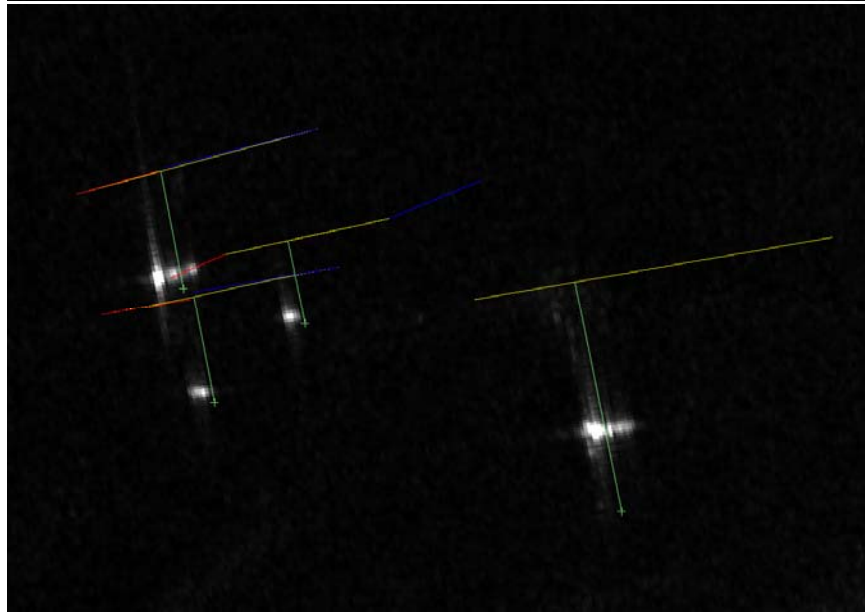
Figure 5. This R-1 SCNB image chip acquired over Gibraltar on 24 July 2006 illustrates the dead-reckoning of the bracketing AIS-snapshots (blue and red lines), the interpolation to AIS-projected position (intersection of green and yellow lines), and the azimuth-shift operation (green line) to the AIS-predicted position (+ sign). Note that the middle vessel is reporting a heading nearly 180° from its actual course, while the rightmost vessel is reporting a speed of zero. The dead-reckoning using a single AIS-snapshot (a) leaves ambiguity in all but the lower left vessel, while the interpolation (b) allows us to calculate reasonable predicted positions, allowing all four vessels to be distinguished with a high degree of confidence.

4.3   Ship Signature Position

To locate the target signature position, a local subscene (equivalent to 800 m by 800 m) centered on the AIS-predicted position is ingested. The position of the maximum σ° value in the subscene is defined as the target signature position; the local subscene is then re-centered on the target signature position for subsequent calculations, including estimation of the total RCS.

4.4   Data Filtering

To ensure that the local subscene containing the matched AIS target signature does not contain land cells, multiple target signatures, and/or other undesirable effects, various filtering techniques were developed to maximize the desired scenario of a single target signature surrounded by representative local ocean clutter. The following provides a synopsis of the target filtering techniques:

- Valid IMO – A target is excluded if the IMO is invalid;

- Land Masking – A target is excluded if there is any land within a 1.6 km radius of the target position;

- Port Masking – A target is excluded if the target position is within a known defined port region where the potential for multiple targets within the local subscene is very high;

- Image Edge Masking – A target is excluded if any part of the desired target subscene is beyond the dimensional constraints of the image product;

- Airball Masking – A target is excluded if any part of the desired target subscene contains image border "airballs" (i.e., the zero padded region around the image);

- Multi-Signature Target Masking – A target is excluded if the target subscene contains multiple signature targets[2] ;

- Multi-AIS Target Masking – A target is excluded if more than one AIS record has been associated with the same signature target;

- Insignificant Target Signature Masking – A target is excluded if

$$\sigma^\circ{}_{max} \leq \left(\bar{\sigma}^\circ{}_{clut} + 5\sigma^\circ{}_{clutSTD} \right)$$

  where $\sigma^\circ{}_{max}$ is the maximum σ° value in the target subscene, $\bar{\sigma}^\circ{}_{clut}$ is the mean of the local ocean clutter, and $\sigma^\circ{}_{clutSTD}$ is the standard deviation of the local ocean clutter;

- AIS-ISR Match – A target is excluded if given the target AIS IMO there is no matching IMO in the ISR database;

- Total RCS ≤ 0 Mask – A target is excluded if the total RCS calculation is ≤ 0;

---

[2] Detecting multiple targets consists of calculating four mean clutter values from each of the four corners in the target sub-scene. A multiple target is sensed if the difference between the maximum mean clutter value and the minimum mean clutter value among the four corners is greater than 5 dB.

- ISR shiplength ≤ 0 Mask – A target is excluded if the ISR shiplength ≤ 0 (i.e., an erroneous ISR entry);

- Search Radius > 400 m Mask – A target is excluded if the spherical distance between the predicted position and the target signature position is greater than 400 m.

In the 23 R-1 SCNB/AISLive data sets, a total of 4965 within-image AIS targets were obtained from the AISLive data. After data filtering operations such as land masking, a total of 1805 high confidence matches between AIS-predicted positions and the associated target signatures are available for further analysis. The target filtering specifics are as follows:

- Total #AIS records within RADARSAT coverage   4965
- # AIS records with IMO < 0   0
- # AIS records with IMO = 0   360
- # AIS records with IMO = 1   0
- # AIS ships landmasked   2436
- # AIS ships portmasked   142
- # AIS ships at image edge   15
- # AIS ships with airballs   53
- # AIS ships with multitargs detected in target subscene   74
- # AIS ships with multiple AIS hits at same target position   13
- # AIS ships with no significant target signature   3
- # counts where no AIS to ISR match occurred   37
- # aistargtotalrcs ≤ 0   6
- # ISR lengths found ≤ 0 meters   7
- # AIS ships with signiftargsig > search radius of 400m   14
- # AIS ships with signiftargsig ≤ search radius of 400m   1805

To illustrate the effects of the filtering operations, Figure 6 shows the AIS-predicted positions for an image acquired over Dover on 2 August 2006 prior to any filtering, while Figure 7 shows the target signature positions after filtering.
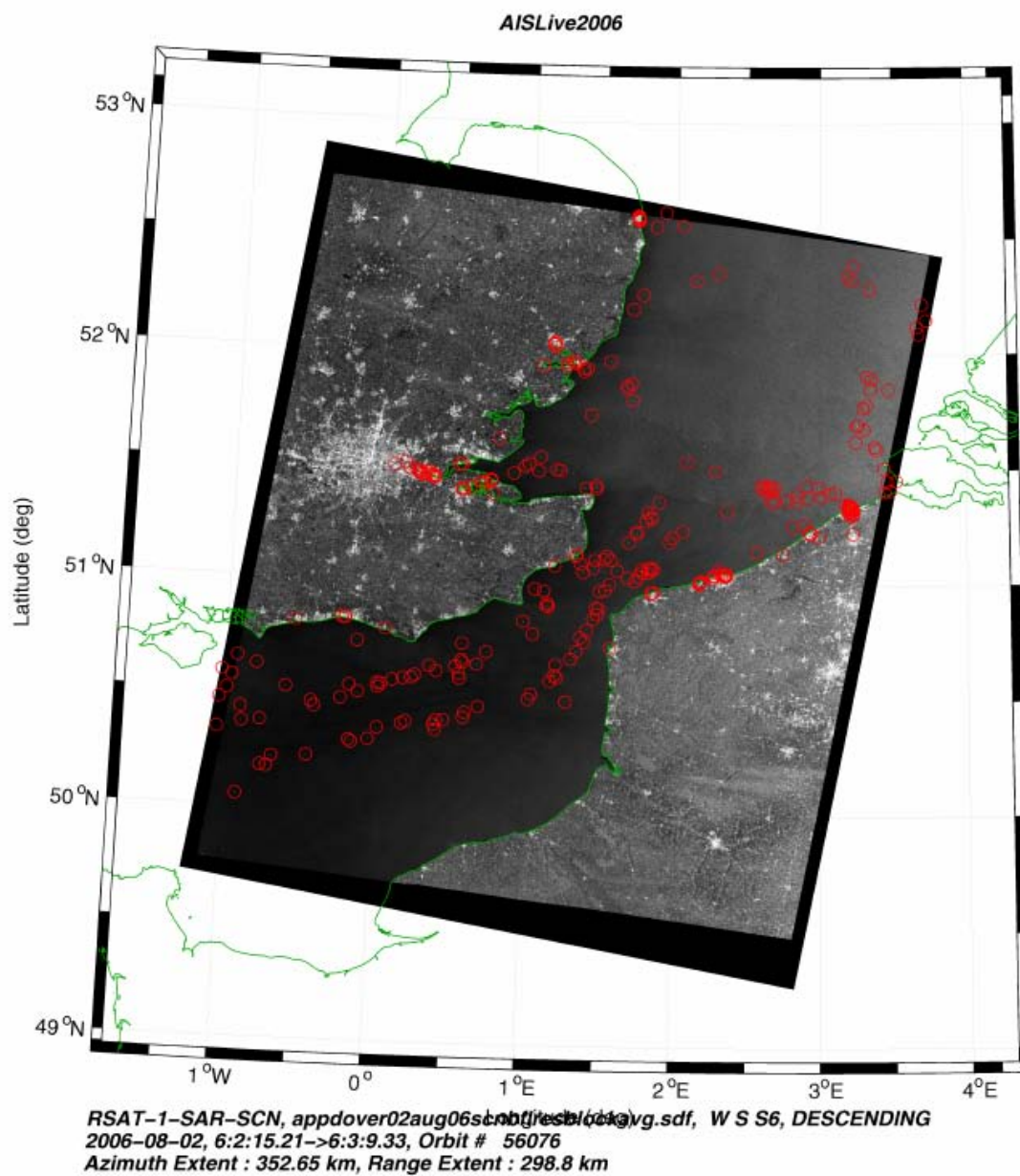
Figure 6. AIS-predicted positions prior to land masking and other filtering operations for the R-1 SCNB image acquired over Dover on 2 August 2006.
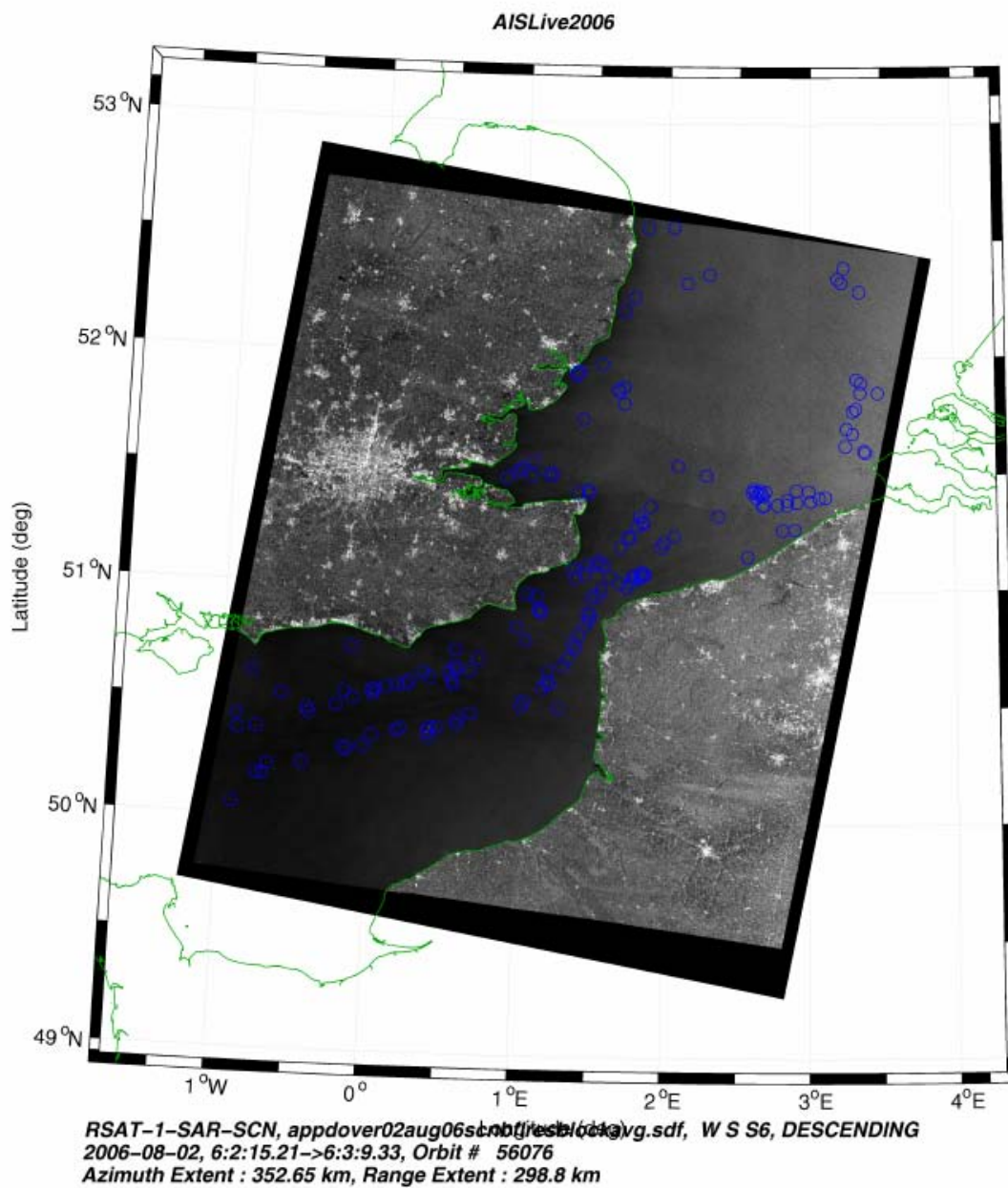
Figure 7. Target signature positions after land masking and other filtering operations for the R-1 SCNB image acquired over Dover on 2 August 2006.

5. Error Analysis of AISLive Data

5.1 Ground Truth

The ground truth for our ATR analysis was actually derived from the Lloyd's Registry Fairplay ISR database, as determined by the vessel identifiers extracted from the AISLive database snapshot service that corresponded with the R-1 image acquisitions. That is, the raw AIS broadcast data were not collected and are not available to us. The results of this error study depend as much on the validity of the two filtering databases as on the original AIS data itself.

AISLive collects AIS broadcast data and updates its database accordingly, including the collation of static, voyage, and dynamic data into a single time-stamped entry. Lloyd's Registry also modifies its ISR database entries over time, as commercial events occur, and is impacted by changes in ownership, flag, and name, to name a few. Having noted this, the ISR and AISLive databases are two independent sources of data and, where agreement occurs, the chance of simultaneous, identical errors is thought to be remote.

5.2 Ship Identification

In the 23 R-1 SCNB/AISLive data sets, 3686 within-image AIS targets with unique identifier sets (IMO, MMSI, Call Sign, and Vessel Name) have been obtained from the AISLive data. Forty-seven of these targets do not appear in the ISR database under any of the noted identifiers. Most of these have been identified as a vessel type not regulated by the IMO, and therefore not part of the ISR collection, e.g., law-enforcement, military, harbour tug, pilot boat, inland-waterway vessel, or domestic ferry. This reduces the number of comparable targets to 3639 vessels.

Comparing the alphanumeric contents of the IMO, MMSI, and Call Sign fields, 3445 of the vessels (94.7% of the 3639 vessels) have completely identical entries (alphanumerically) for the 3 fields in both databases. Of the 196 remaining vessels, 44 have either the MMSI or Call Sign (or both) missing from the ISR database. At most, 152 of the vessels (4.18% of the 3639 vessels) might have errors in their AIS identifier information. It is expected that non-error differences, such as the sale, renaming, and issue of new identifiers, will reduce this estimate. It should be noted that there is only one vessel for which both the IMO and the Call Sign have ISR entries but cannot be matched alphanumerically to the AISLive fields. In this case, the IMO number in the AISLive data has a 1-digit error, while the Call Sign is completely different.

Since the MMSI, Call Sign, and Vessel Name can legitimately change over time, it is difficult to distinguish differences in these fields due to AIS errors from database latency or other non-error effects. The IMO, on the other hand, remains the unique identifier for a hull throughout its lifetime. Thus, differences between the AISLive and ISR databases should be indicators of error. To this end, 34 cases (0.934% of the 3639 vessels) for which the AISLive IMO data is in error (taking the ISR database as the truth) have been observed, see Table 2.

Table 2. Enumeration of observed IMO Errors.

Error Class	Error Type	Number of Errors
Transcription	1-digit dropped	5
	1-digit miskeyed	11*
	2-digits miskeyed	1*
	2-digits transposed	1
Invalid Number	Entered as 0	1
	Entered first 3 digits only	2
Incorrect Number	Official Number used	6
	Transposed with MMSI	2
	Entered as 8888888	1
	Unknown error	4
Total		34

*In two cases, the error points to an incorrect ISR database entry; the resulting IMO belongs to another vessel.

5.3   Ship Length

The vessel length according to the ISR Database was compared to that reported via AIS, as shown in Figure 8. Most of the AIS errors correspond to reports of zero ship length, and there are several cases of incorrectly populated fields (e.g., it appears that the ship width was reported rather than the length). Overall, an error rate is evident in the AIS-reported length of about 9.92%, where an error is generously defined as a discrepancy between the two length measures of 30% or more. For subsequent analysis, the actual vessel length was taken as the verified length according to the ISR Database.

Figure 9 shows a histogram of the ISR ship length with mean and standard deviation equal to 147 m and 66 m, respectively. The minimum and maximum ship lengths for the data set are 40 m and 350 m, respectively.
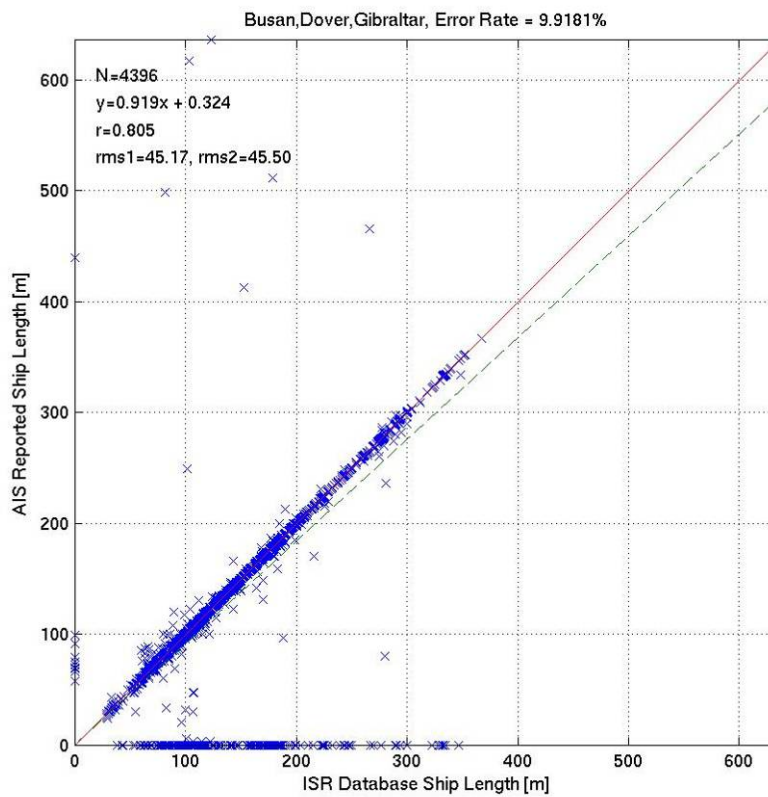
Figure 8. Scatter plot of the ship length according to the ISR database and as reported via AISLive.
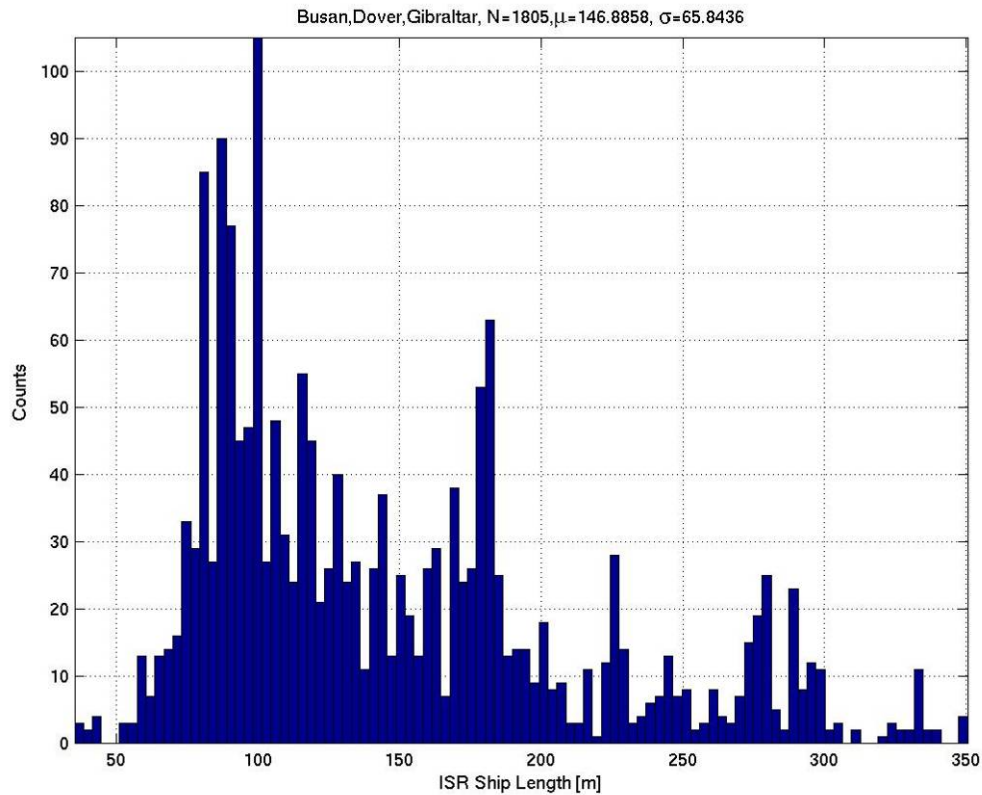
Figure 9. Histogram of the ISR database ship length for the R-1 SCNB dataset.

5.4   Dynamic Data

By using bracketing AISLive snapshots, the only AIS dynamic data used in the subsequent analysis is the GPS position information. The two positions and their acquisition times allow CoG and SoG to be estimated independently, as per Section 4.1, from the AIS-supplied fields for heading, CoG, and SoG.

It would be preferable to be supplied with both AIS Heading and AIS CoG for all cases; AISLive has been informed of this, but has not altered their snapshot format, which provides AIS CoG only when AIS Heading is unavailable. As for the preference for AIS CoG over AIS Heading, for ships traveling at significant speeds, say > 5 knots, the AIS CoG becomes important for single AISLive observations since the CoG is the basis for calculating the DR and the velocity component for the azimuth shift of the SAR-imaged ship signature. For stationary targets, that is moored, anchored, or station-keeping, where speeds are low, say < 0.5 knots, the AIS CoG becomes a random-walk dominated by noise and is of little value.

Since we do estimate an independent CoG when pairs of snapshots are available, we can compare the estimated CoG against the provided AIS Heading to estimate the magnitude of errors arising from using the AIS Heading instead of an actual CoG (see Figure 10). Following data filtering operations such as land masking, 1452 cases with pairs of AISLive snapshots remained for this analysis, amounting to 2904 separate comparisons of estimated CoG and provided AIS Heading.

The mean error of this comparison is 48 m with a standard deviation of 143 m, which is less than the length of many of the vessels under consideration. Only 39 of these comparisons (1.34% of the 2904), representing 28 different vessels, exhibit a position error that is greater than the SAR signature proximity distance that was used, i.e., 500 m (recall that we are working with pairs of snapshots; in some cases only one of the possible two comparisons exceeded the SAR signature proximity distance). Three of the vessels are involved in manoeuvring (as judged by comparing the change in AIS Heading with the estimated CoG), which likely generates the discrepancy. Three additional vessels exhibit an AIS SoG that cannot be reconciled with the AIS positions (in two comparisons there was zero speed reported, but the vessel position changed significantly; in one comparison the speed was reported as 11.2 knots, but the vessel position did not change). The difference between AIS Heading and interpolated CoG is given for the remaining 22 pairs (see Figure 11), showing an unbiased distribution. Statistically, it appears that the use of AIS Heading and AIS SoG to dead-reckon positions where only one AISLive snapshot is available, is appropriate, and will have little impact on the ability to match AIS validation data with SAR image signatures.
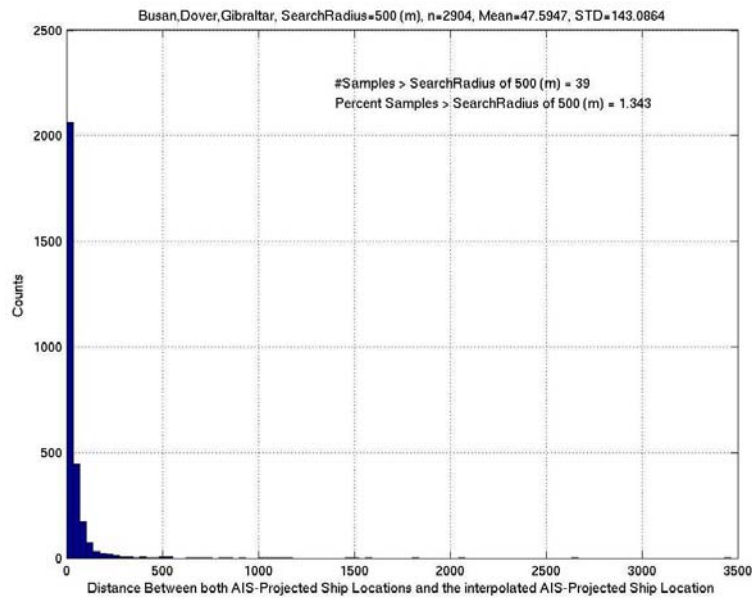
Figure 10. Histogram of the spherical distance between AIS-projected positions derived from AIS Heading/SoG and interpolated CoG/SoG.
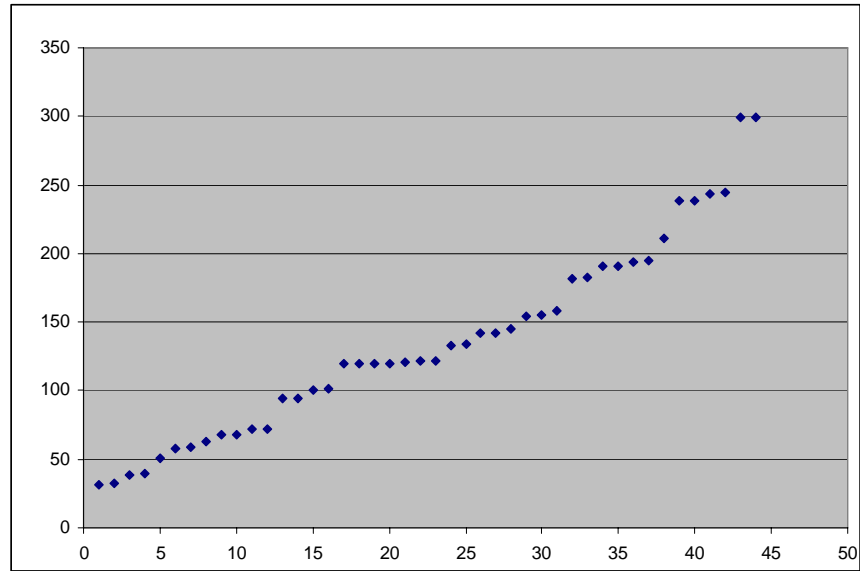

Figure 11. Difference between AIS Heading and interpolated CoG for outlier ships.

6. Examples of Matched AIS and Ship Target Signatures

This section shows some illustrative examples that are intended to provide a visual and statistical link between the target signature in the SAR image and the matched ship in the AIS data. They also illustrate some of the dynamics of the dataset. Each figure consists of the SAR sub-scene underlay with the target signature identified, a photograph of the vessel in question, the associated AISLive snapshot parameters, and the ship signature point-target analysis results from the VUSAR tool. Figure 12 and Figure 13 show the vessels with the minimum and maximum ship lengths found in the entire dataset. Figure 14 and Figure 15 show the vessels with the minimum and maximum total RCS found in the entire dataset. Meanwhile, Figure 16 shows a vessel that had essential the mean length and the mean total RCS found in the entire data set.
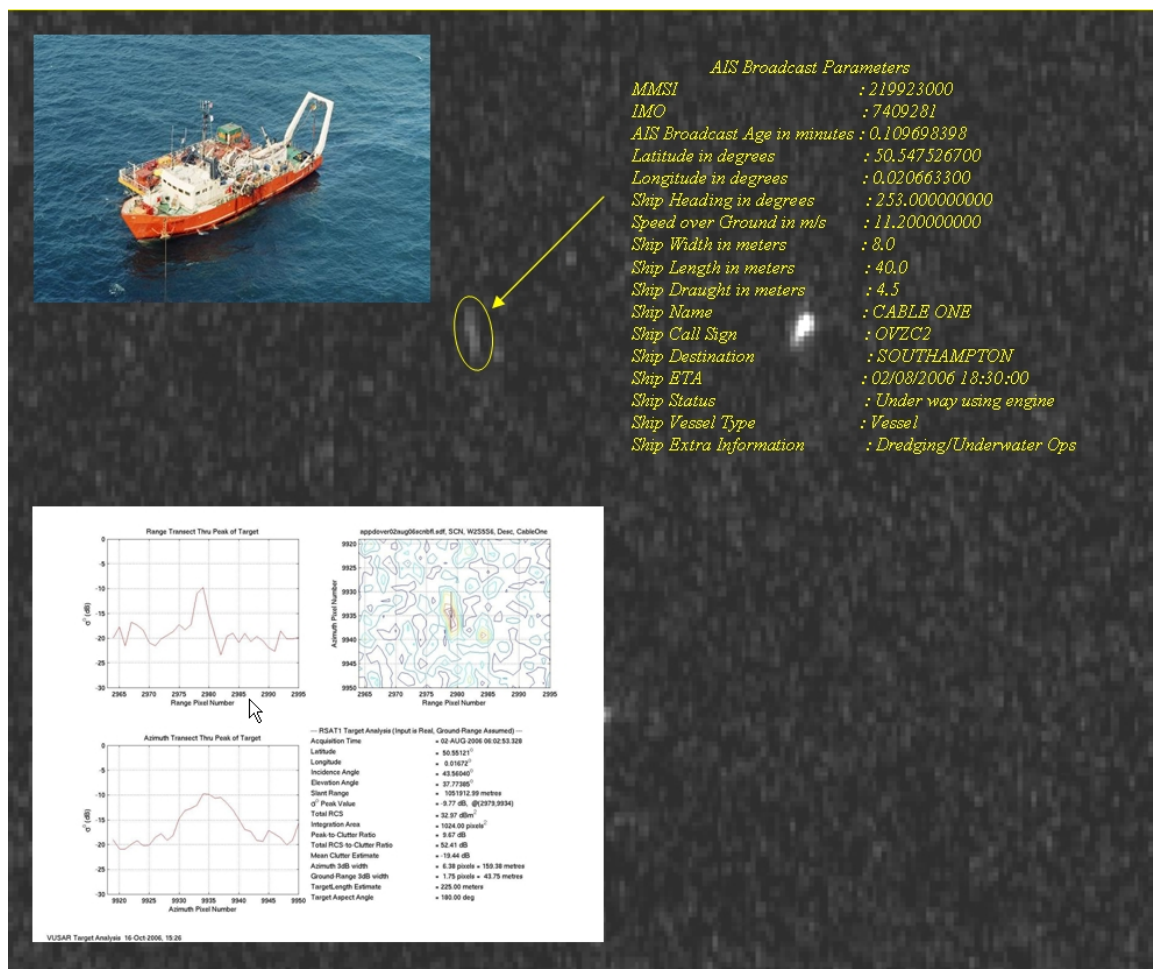
Figure 12. The ship with the minimum ship length in the entire dataset. The Cable One is a dredging vessel with an overall length of 40 meters and had a measured total RCS of 32.97 dB-m^2. Ship photo courtesy of www.fotoflite.com.

Figure 13. The ship with the maximum ship length in the entire dataset. The Cosco Hellas is a container ship with an overall length of 351 meters and had a measured total RCS of 59.96 dB-m². Ship photo courtesy of www.fotoflite.com.
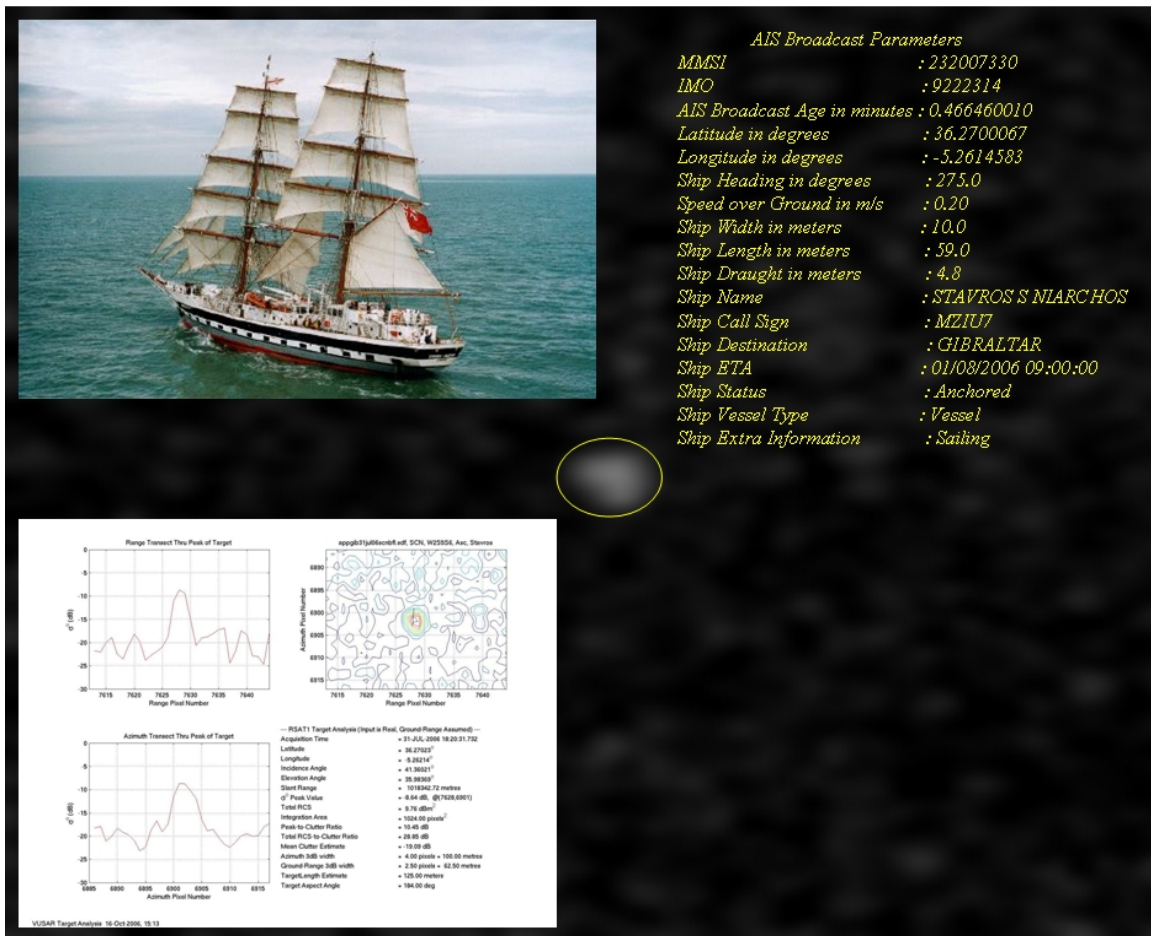
Figure 14. The ship with the minimum measured total RCS in the entire dataset. The Stavros Niarchos is a sailing vessel with an overall length of 59 meters and had a measured total RCS of 9.76 dB-m². Ship photo courtesy of www.fotoflite.com.
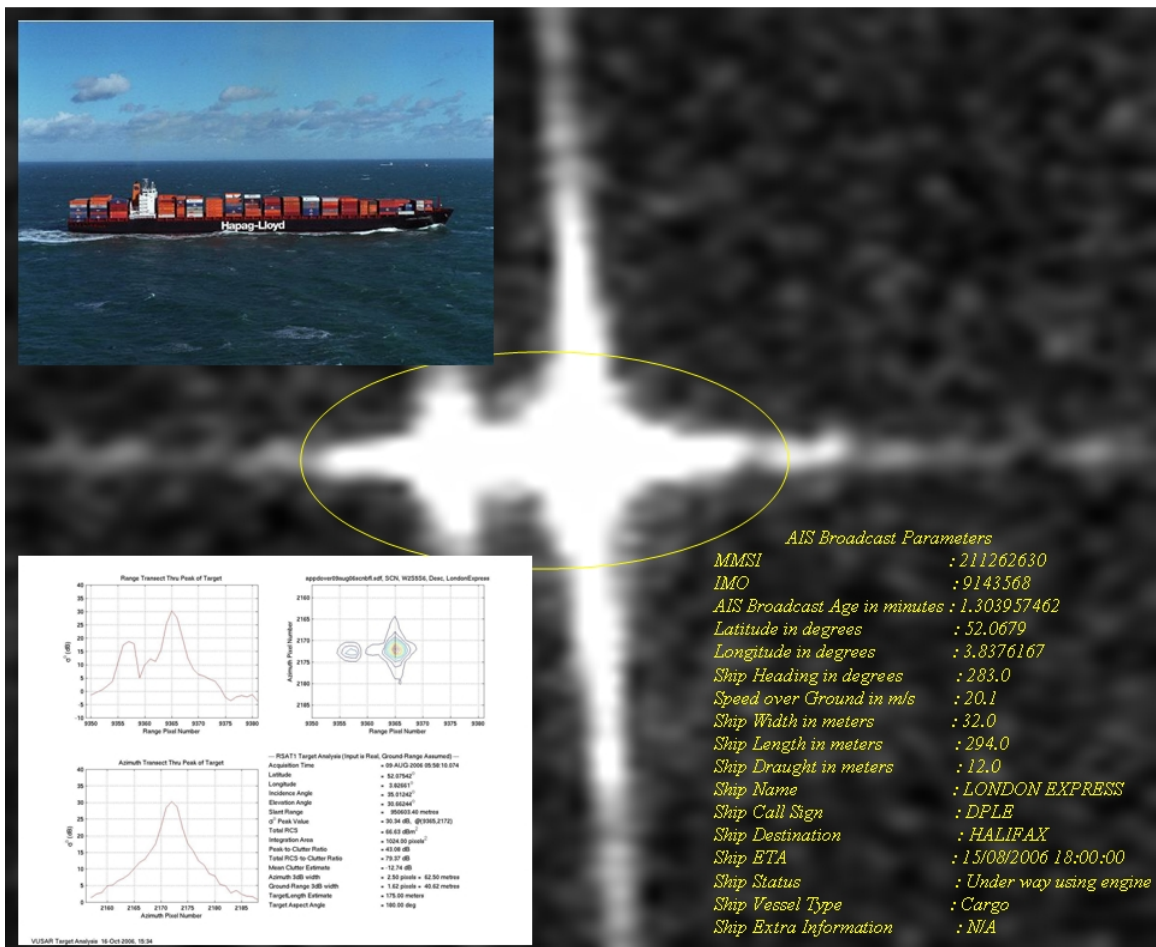
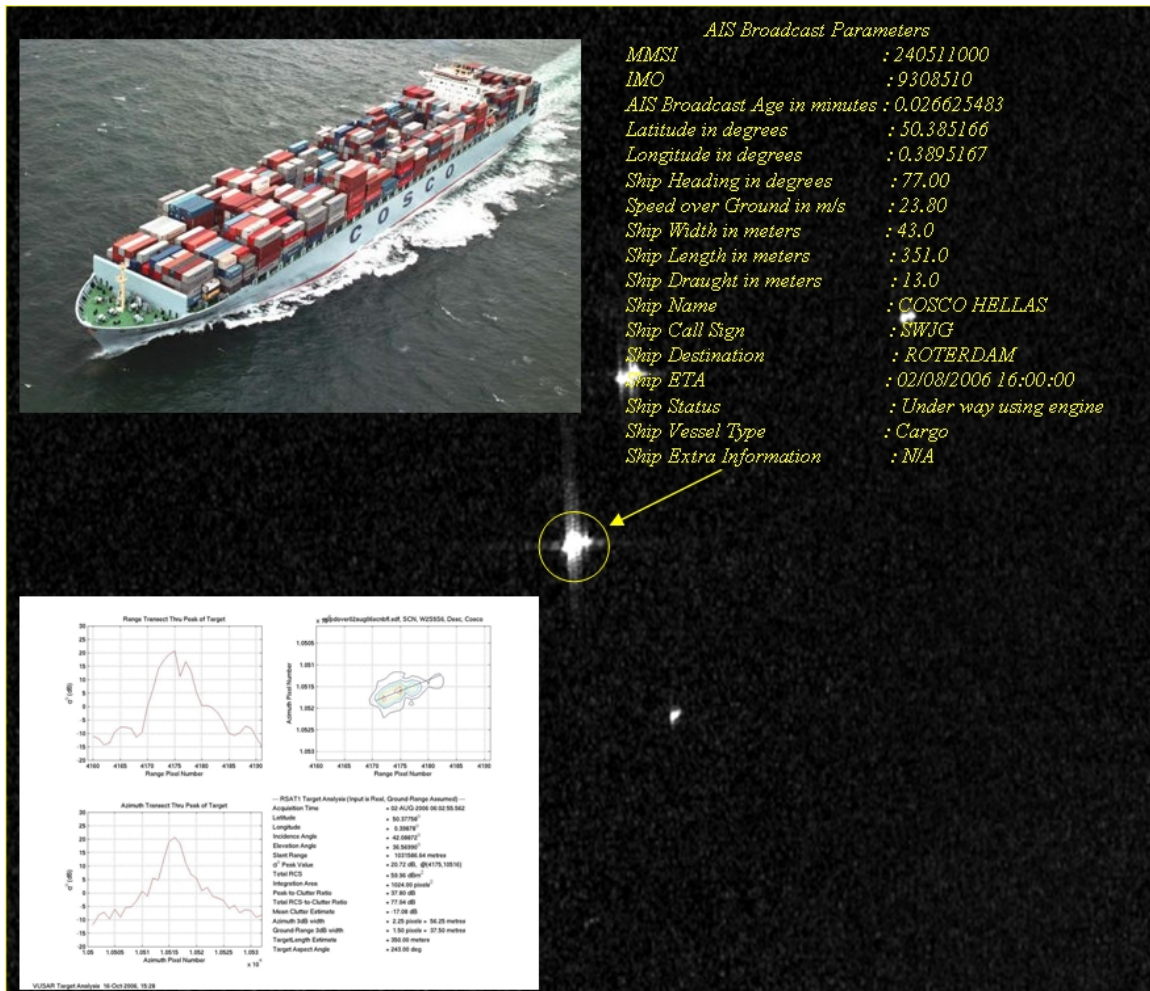*Figure 15. The ship with the maximum measured total RCS in the entire dataset. The London Express is a container ship with an overall length of 283 meters and had a measured total RCS of 66.63 dB-m². Ship photo courtesy of www.fotoflite.com.*

Figure 16. A representative ship that measures very close to the overall mean ship length and overall mean total RCS for the entire dataset. The Saramati is a cargo ship with an overall length of 146 meters and had a measured total RCS of 46.83 dB-m^2. Ship photo courtesy of www.fotoflite.com.
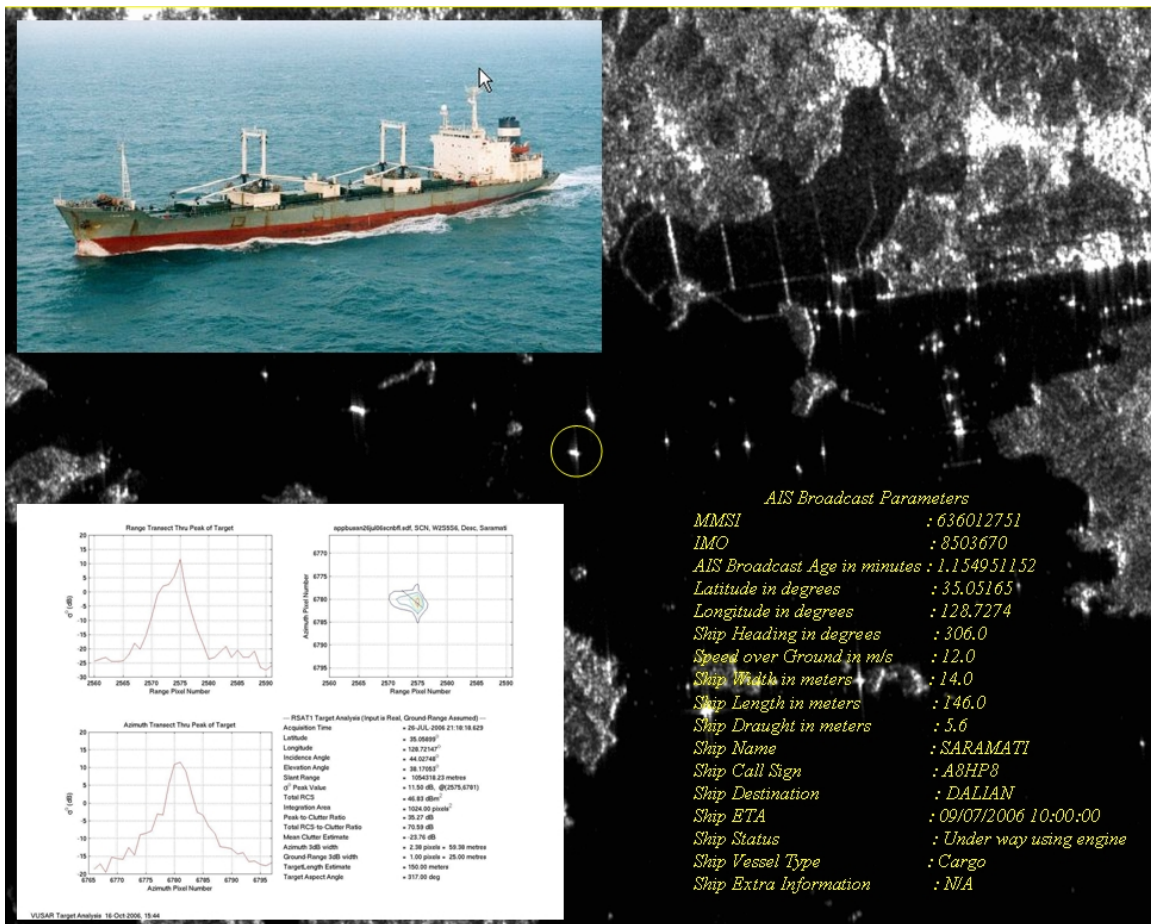
7.   Ship Signature Analysis

7.1   Position

The improvement in the position accuracy provided by the dead-reckoning/interpolation and the azimuth-shift operations is illustrated by Figure 17 through Figure 19. Figure 17 shows a histogram of the absolute difference between the AIS-*reported* positions and the target signature positions. Figure 18 shows a histogram of the absolute difference between the AIS-*projected* positions and the target signature positions. Figure 19 shows a histogram of the absolute difference between the AIS-*predicted* positions and the target signature positions. Table 3 summarizes the results by providing the mean and standard deviation of the separation distances[3] between the AIS reported, projected, and predicted positions and the target signature positions. The mean separation distance is reduced from 638.5 m for the AIS-reported position to 124.2 m for AIS-predicted position, which is smaller than the average ship length in the data set. The standard deviation of the separation distance is reduced from 460.8 m for the AIS-reported position to 66.5 m for the AIS-predicted position.

Figure 17. Histogram of the separation distance between the AIS-reported ship position and the target signature position.

---

[3] The separation distance is the spherical distance between the AIS-position (where position is one of reported, projected or predicted) and the maximum $\sigma°$ location in the target signature.

Figure 18. Histogram of the separation distance between the AIS-projected ship position and the target signature position.
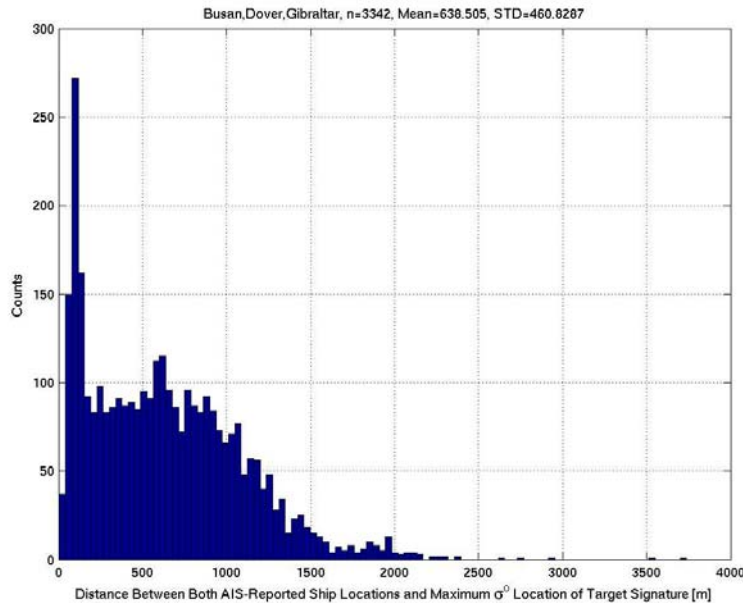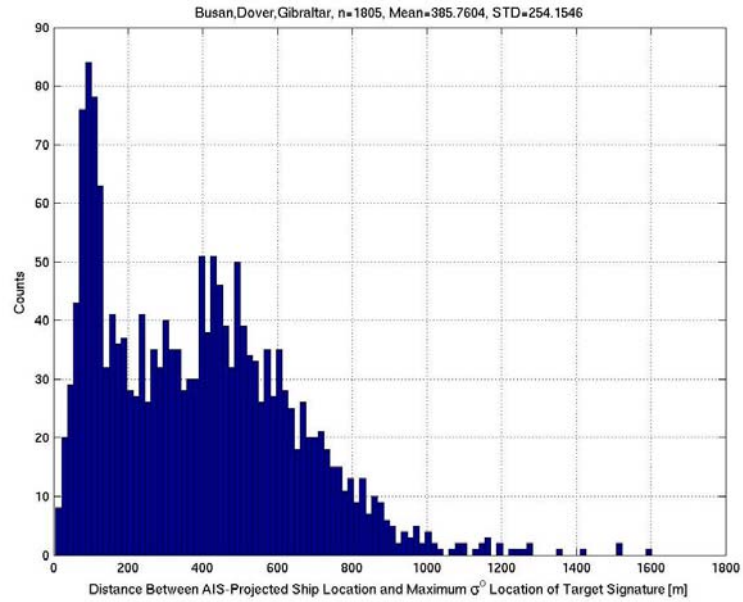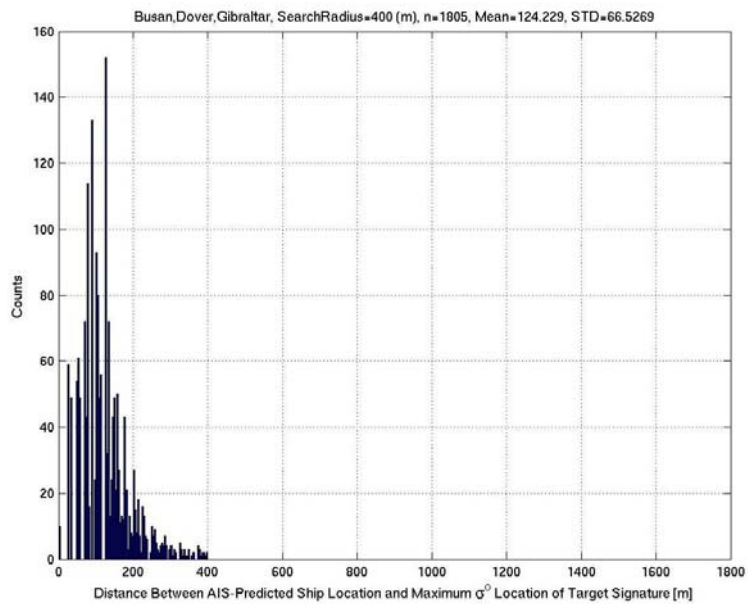

Figure 19. Histogram of the separation distance between the AIS-predicted ship position and the target signature position.

Table 3. Comparison of AIS Position and Target Signature Position.

AIS Position	Mean [m]	STD [m]
Reported	638.5	460.8
Projected	385.8	254.2
Predicted	124.2	66.5

7.2   Radar Cross Section

We now have available a data set that is amenable to assessment of automatic analysis tools, providing a good set of well-separated target vessel signature for which there is a high confidence in the accuracy of vessel ground-truth data. For purposes of this document, the primary measures considered are the ISR ship length and the estimated total radar cross section (RCS) of the matched ship target signature using the VUSAR tool. Figure 20 provides a histogram of the total RCS, indicating an overall mean of 44 dB-m^2.

Figure 21 shows a log-log plot of the VUSAR-measured total RCS versus the validated ISR Database ship length. A simple fit to the observed data is given by:

$$\sigma_S = 0.324L^{2.3} \tag{5}$$

where σ_s is the total RCS in m^2 with the sub-script "S" referencing the ScanSAR mode source of the SAR data, and L is the ship length in meters. There is considerable dispersion about this model fit since target geometry (i.e., the incidence and aspect angles), the target type, and the vessel configuration have not been accounted for. Figure 22 shows a histogram of the total RCS following normalization by σ_s. The fit of equation (5) is also referred to as the "AISLive2006" fit.

As a check for incidence angle dependence, the total RCS normalized by σ_s was plotted as a function of incidence angle. The data span incidence angles from 31° to 48° (recall that the R-1 data were all SCNB mode in this case). No dependence on incidence angle was found.
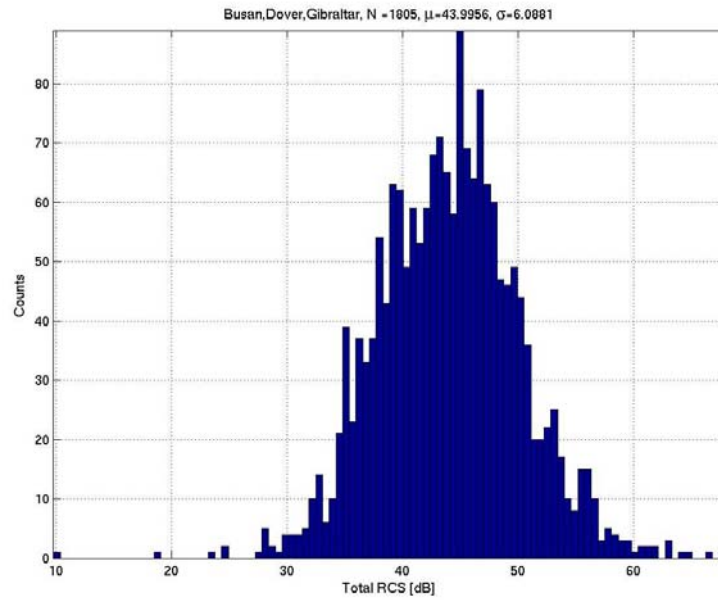
Figure 20. Histogram of the Total RCS for the R-1 SCNB dataset.
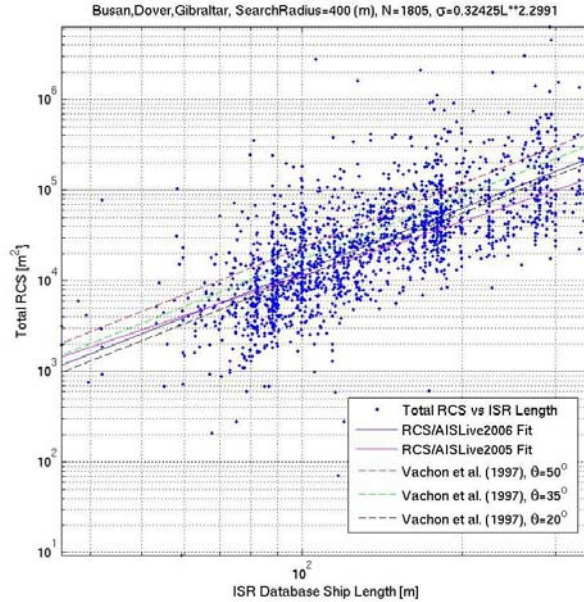
Figure 21. Log-log plot of the VUSAR-measured Total RCS versus the validated ISR Database ship length along with several model fits.

Busan,Dover,Gibraltar, SearchRadius=400 (m), n=1805

Mean=1.897448
STD=5.718878
Mean²/Var=0.110083
Skewness=21.423594
Kurtosis=636.028834
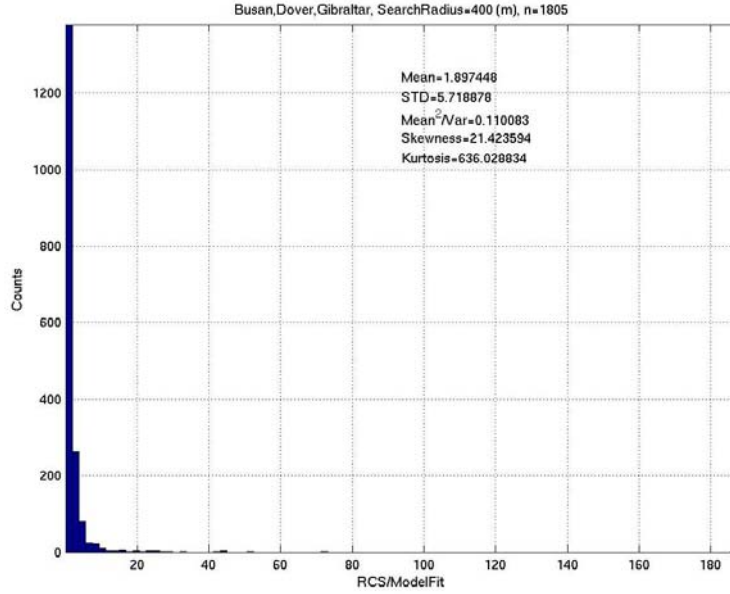
Figure 22. Histogram of the normalized Total RCS for the R-1 SCNB dataset.

Figure 21 compares our observed RCS values with two other models for ship RCS that are available. First, Vachon *et al.* [9] suggested the following formula for ship RCS:

$$\sigma_V = 0.08 L^{7/3}(0.78 + 0.11\theta) \tag{6}$$

where σ_V is the total RCS in m² and θ is the incidence angle expressed in degrees. This empirical model is based upon comments by Skolnik [6] concerning ship RCS and used a very limited number of known ships in R-1 single beam mode data. Second, Vachon et al. [8] used R-1 Fine mode data and AISLive data acquired in 2005 for validation to arrive at the following formula for ship RCS:

$$\sigma_F = 1.25 L^{1.98} \tag{7}$$

with the sub-script "*F*" referencing the Fine mode source of the SAR data. The fit of equation (7) is also referred to as the "AISLive2005" fit. Each of the models appears to be similar to the total RCS values derived from the SCNB data.

7.3   Probability Density Function

In order to model the dispersion of the observed total RCS data derived from SCNB, as was done in [10] for Fine mode data validated with AISLive data, the well-known Kolmogorov-Smirnov Hypothetis (KSH) [3][4] was used to judge the quality of fits of the normalized RCS to standard probability density function (PDF) models including Gamma, Rayleigh, Rician, Weibull, Chi-squared, and Log-Normal distributions. Much more effort could be put into this type of analysis, based upon more complex, multi-parameter PDFs (e.g., [2]). However, only the Log-Normal distribution showed promise (i.e., was accepted by the KSH test), thus becoming the focus of this analysis.

Figure 23 and Figure 24 show PDF and CDF plots of the normalized RCS for all 1805 ships in the SCNB dataset, along with the associated Log-Normal fits. For each such plot, the actual data are represented by the bar graph and the solid black line; the fitted PDF is represented by the solid red line; the parameter fits are shown in the legend; and the KSH test result is shown on the plot. In this case, it is noted that the Log-Normal PDF fit to this data set is rejected by the KSH test.

Figure 25 through Figure 31 provide the PDF plots of the normalized RCS stratified across various ship length populations. Table 4 provides a summary of the results showing the ship lengths, the KSH test result, the number of samples per population considered, and the shape (A) and scale (B) parameters for the Log-Normal distribution fit. We see that a suitable fit is not found across the entire data set, but when stratified by ship length, the Log-Normal distribution can be used in some cases to model the observed total RCS variability.
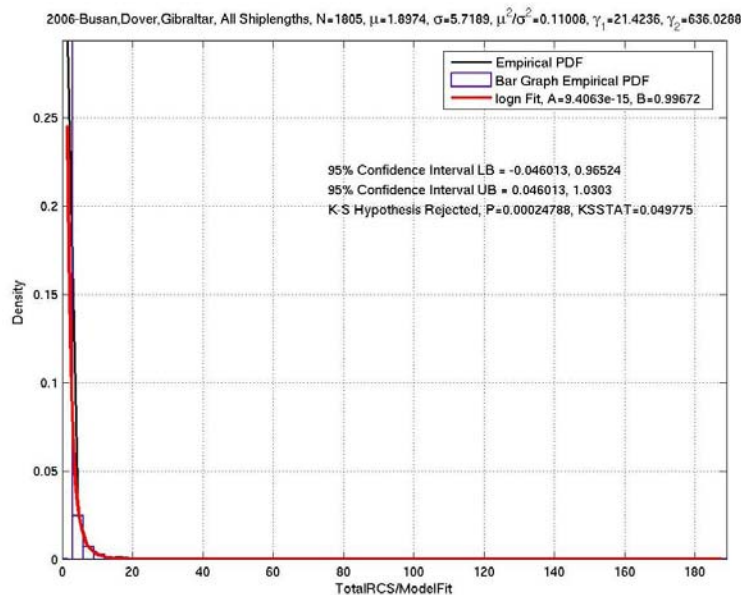
Figure 23. PDF of the normalized RCS for the entire dataset with a Log-Normal PDF fit.
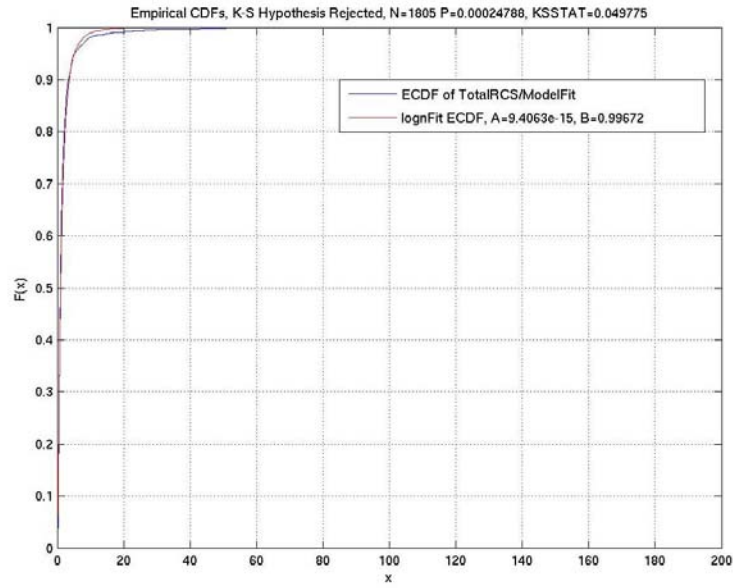
Figure 24. CDF of the normalized RCS for the entire dataset with a Log-Normal CDF fit.

Table 4. Summary of Log-Normal PDF fits to various ship length sets.

Ship Length [m]	L<75	75≤L<125	125≤L<175	175≤L<225	225≤L<275	275≤L	100<L<300
KSH Test	Accepted	Rejected*	Accepted	Accepted	Accepted	Accepted	Rejected
# Samples	101	773	385	284	123	139	1179
A	0.013448	--	0.10402	0.11548	−0.21239	−0.090188	--
B	1.2167	--	0.90716	0.90787	0.9845	1.0637	--

*Removing the two largest normalized RCS values results in KSH being accepted, with # Samples = 771, $A = -0.054282$, and $B = 0.99468$.
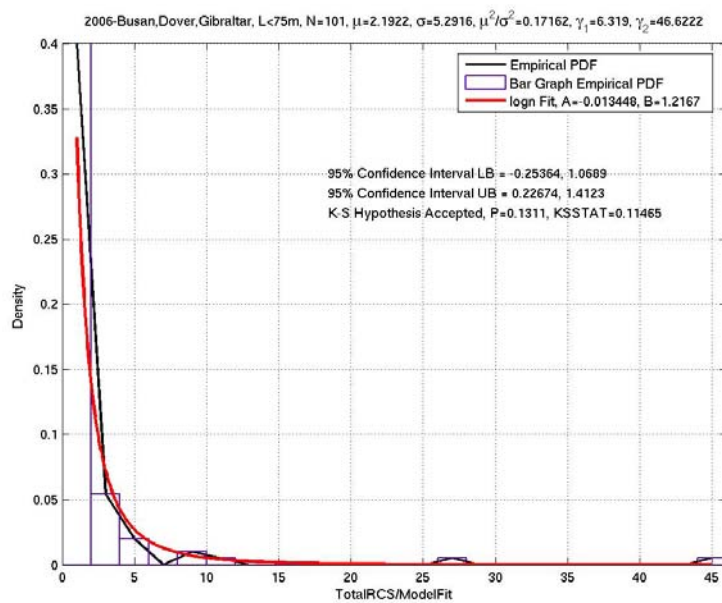
Figure 25. PDF of the normalized RCS for L < 75 m with a Log-Normal PDF fit.
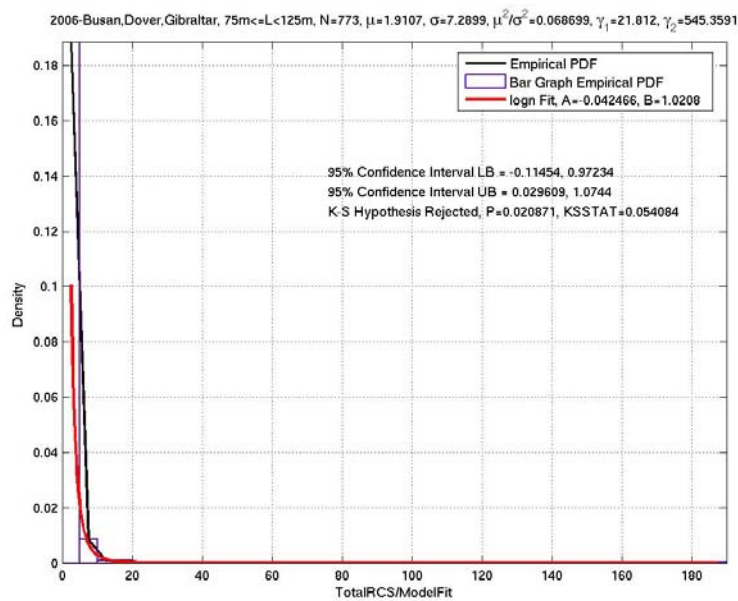
Figure 26. PDF of the normalized RCS for 75 m ≤ L < 125 m with a Log-Normal PDF fit.
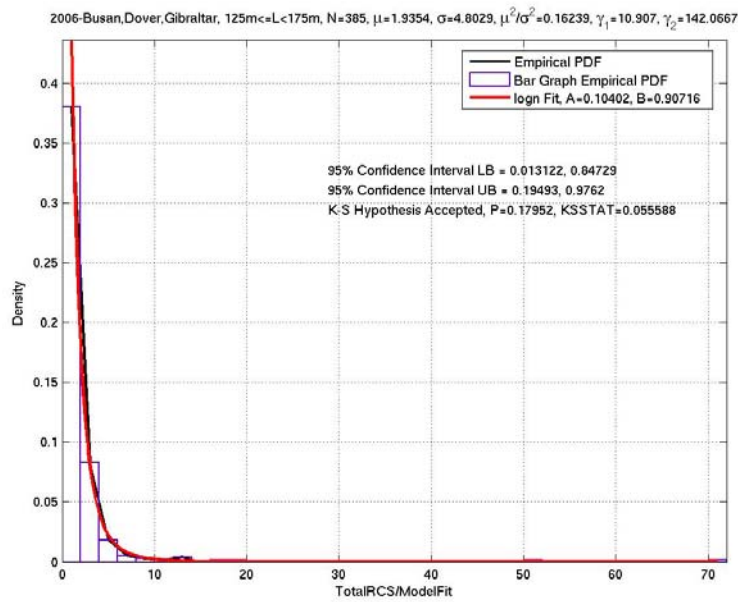
Figure 27. PDF of the normalized RCS for 125 m ≤ L < 175 m with a Log-Normal PDF fit.
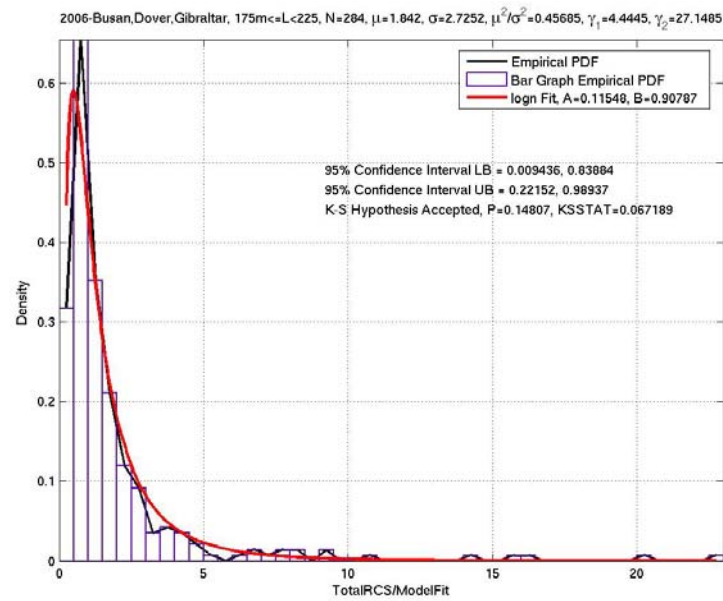
Figure 28. PDF of the normalized RCS for 175 m ≤ L < 225 m with a Log-Normal PDF fit.
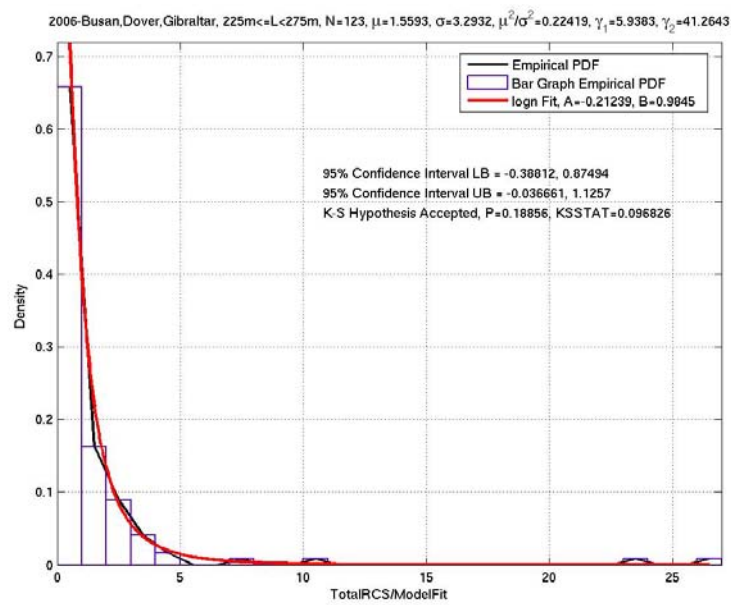
Figure 29. PDF of the normalized RCS for 225 m ≤ L < 275m with a Log-Normal PDF fit.
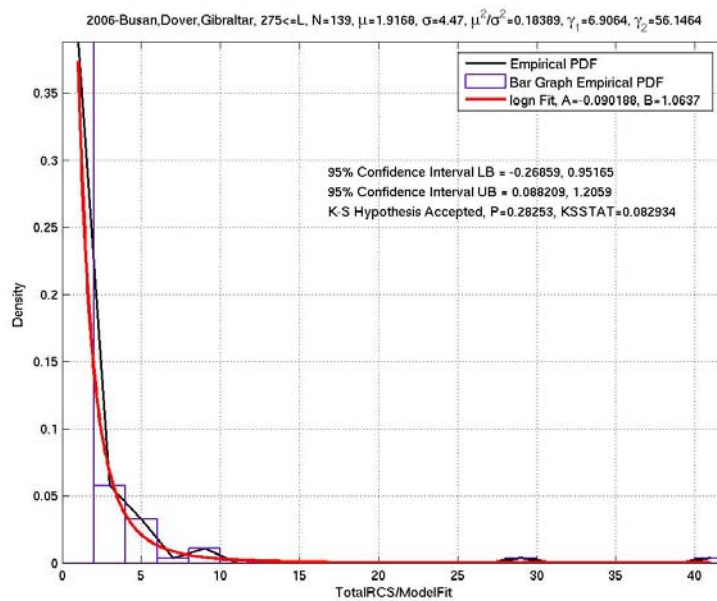
Figure 30. PDF of the normalized RCS for 275 m ≤ L with a Log-Normal PDF fit.
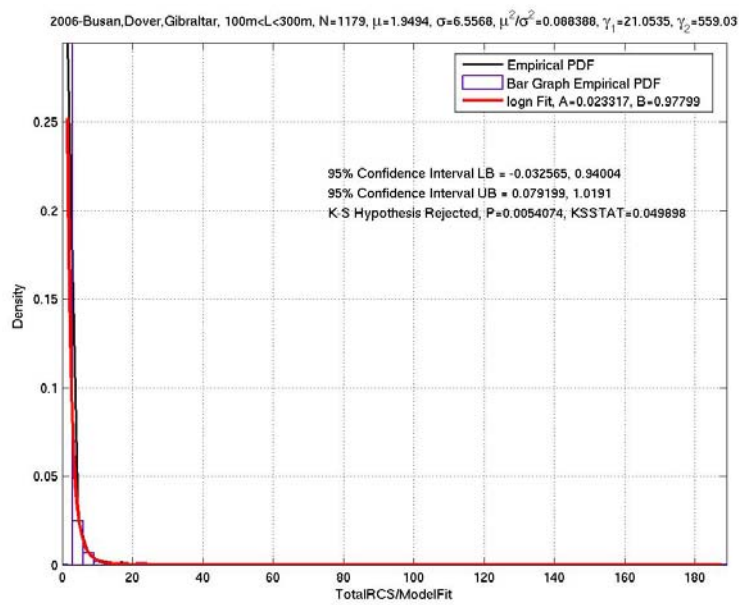
Figure 31. PDF of the normalized RCS for 100 m < L < 300 m with a Log-Normal PDF fit.

8.   Comparison of the 2005 and 2006 Datasets

The document has focussed on the analysis of 1805 ship signatures in SCNB mode data acquired in 2006, as validated with AISLive data. A similar data set was acquired in 2005, but based upon 399 ship signatures in Fine mode data. A key question is whether or not the ship RCS results are consistent between the two data sets. As noted in the previous section, the empirical model fits are slightly, but not drastically, different between the two data sets. If we could combine the two data sets, for example, then it would provide a larger validated ship population for subsequent statistical analysis. Differences between the two data sets could be related to the resolution at which the data were acquired (nominally 50 m for SCNB mode and 8 m for Fine mode).

To compare the two data sets we again used the KSH test, but this time to establish whether or not the Fine mode RCS data set could have been drawn from the same population as the SCNB mode RCS data set. Table 5 summarizes various tests that were performed to examine the behaviour of the test and the comparison of the two RCS populations.

In Test #1, we tested the first half of the SCNB mode RCS data (sample population X1) against the second half of the SCNB data (sample population X2). Likewise, in Test #2, we tested the first half of the Fine mode RCS data (sample population X1) against the second half of the Fine data (sample population X2). In both cases, the KSH is accepted, thus validating the test, indicating internal consistency within the two data sets, and establishing how the test can be used to show that samples have been drawn from the same population.

In Test #3, we tested the Fine mode RCS data (sample population X1) against the SCNB RCS data (sample population X2). In this case, the KSH is rejected, indicating that the two data sets were not drawn from the same continuous population.

In Test #4, we tested the Fine mode normalized RCS data (sample population X1) against the SCNB mode normalized RCS data (sample population X2). In this case, the KSH is accepted, indicating that the two data sets were drawn from the same continuous population. The result is extremely important since it shows that although the normalizations that were used were different in the two cases, the variability of the normalized RCS values was the same. This is in spite of the fact that we were not able to find a simple PDF that described the variability across the full set of either normalized SCNB mode or normalized Fine mode data. Apparently, the difference between the Fine mode and SCNB mode data sets rests in the difference between the two normalization functions.

As a final test, and in spite of the result of Test #4, we went ahead and combined the Fine mode and SCNB mode data sets. In Test #5, we tested the Fine mode RCS data normalized by the combined fit (sample population X1) against the SCNB mode RCS data normalized by the combined fit (sample population X2). In this case, although the combined fit is quite similar to the SCNB fit of equation (5), the KSH is rejected, which affirms that the two RCS populations are different.

Table 5. KSH test results to determine sample population dependence.

Test #	Input Populations X1 and X2 to kstest2	KSH Test
1	X1=First half of SCNB mode RCS data (N=903) X2=Second half of SCNB mode RCS data (N=902)	Accepted
2	X1=First half of Fine mode RCS data (N=200) X2=Second half of Fine mode RCS data (N=199)	Accepted
3	X1=Fine mode RCS data (N=399) X2=SCNB mode RCS data (N=1805)	Rejected
4	X1=Fine mode RCS data normalized by equation (7) (N=399) X2=SCNB mode RCS data normalized by equation (5) (N=1805)	Accepted
5	X1=Fine mode RCS data normalized by combined fit (N=399) X2=SCNB mode RCS data normalized by combined fit (N=1805)	Rejected

In Figure 32 and Figure 33 we compare the normalization functions that were estimated for the Fine mode, SCNB, and the combined data sets. In comparison to the Fine mode normalization function, the SCNB data are different by from −1 dB for smaller ship lengths to 2 dB for longer ship lengths. Since the variability of the normalized RCS data is the same for the Fine and SCNB data sets, we assume that this difference can be ascribed to the resolution of the two beam modes. Although this does not appear to be a large difference, it could be indicative of the resolution dependence of ship RCS and would warrant further investigation.
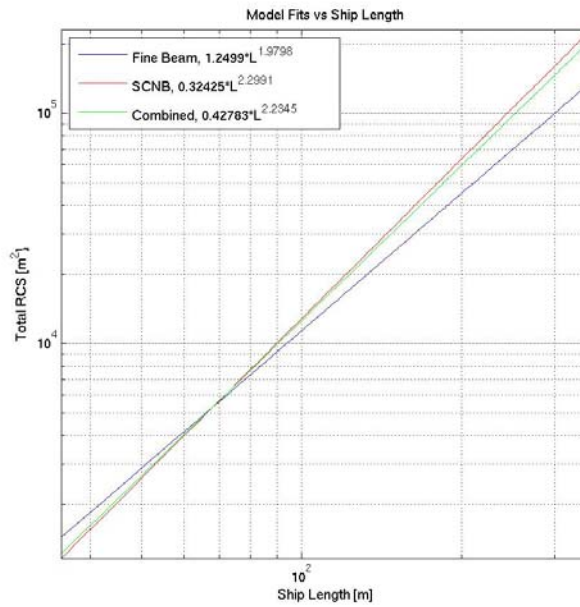
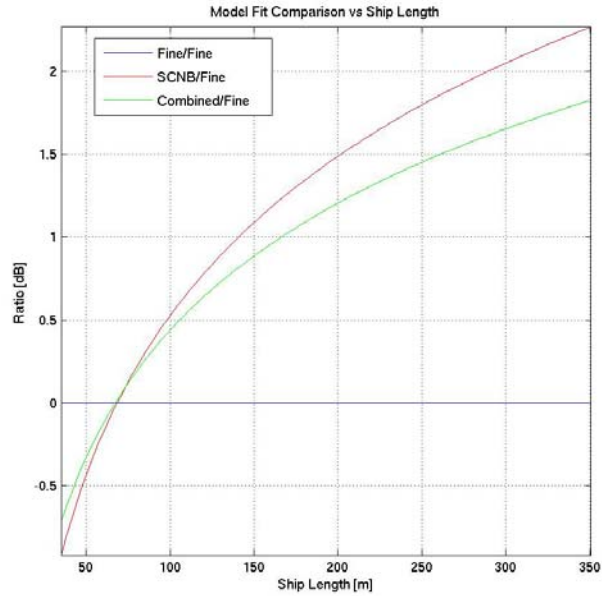*Figure 32. Three model fits for total RCS versus ship length for Fine, SCNB, and Combined data.*

Figure 33. Ratio of the model fits to the Fine mode case versus ship length for Fine/Fine, SCNB/Fine, and Combined/Fine.

9. Conclusions

In this document, the analysis of ship signatures in RADARSAT-1 SCNB imagery in the context of AISLive vessel validation data has been considered. The following conclusions are offered:

- CSIAPS should be used to refine the expected pass time if temporal accuracy is critical to the planning of validation data acquisition. CSIAPS provided predicted pass times within a few seconds of actual if run roughly one week in advance of the acquisition (and provided the orbit data was correctly updated). On the other hand, SPA provided predicted pass times within a few minutes of the actual pass times.

- 8-bit SCNB products from the CDPF will often saturate the available dynamic range, leading to an underestimate of the ship RCS. We overcame this problem by working from floating point products that were generated on a desktop SAR processor. In general, dynamic range saturation is a problem that will limit the quantitative evaluation of ship signatures.

- The AISLive data contains inherent errors relative to an authoritative ship database. These errors might reflect the error rates in AIS data in general. Ship identification errors were relatively rare but do occur. Ship length, a key parameter for our RCS analysis, was in error for nearly 10% of the cases considered. Errors in dynamic data also occur but are more difficult to quantify. Use of bracketing AISLive snapshot data sets reduced dead-reckoning errors that could be associated with single snapshot dead reckoning.

- Interpolation schemes were developed to provide AIS-predicted positions for ships in the SCNB data. The predicted positions included an azimuthal shift operation to account for the Doppler shift associated with moving targets. For the high density shipping regions considered, it was essential to carry out both interpolation and azimuth shifting operations. We found that the error between the AIS-predicted position and the ship signature position (124 m) was smaller than the average ship length in the overall data set (147 m).

- This work resulted in a set of 1805 validated SCNB ship signatures. The ships ranged from 40 m to 350 m in length.

- The total RCS of the SCNB ship data was modelled as a simple geometric function of the ship length according to equation (5). The variability about the normalized RCS, a consequence of ship type, incidence angle, aspect angle, and sea state, to name a few, could not be described by a single PDF, but a Log-Normal distribution does appear to be appropriate for certain ship length ranges. The fitting of the normalized RCS data to more complex, multi-parameter PDFs is warranted.

- The variability of the normalized SCNB ship RCS data considered in this document is the same as the variability of the normalized Fine mode ship RCS data that were acquired in 2005. However, the two data sets differ by the normalization function which amounts to a few dB over the available range of ship lengths. Presumably this difference can be ascribed to the RCS being slightly dependent upon the resolution at which the data were acquired. Further investigation of the resolution dependence of the RCS could lead to new and more accurate ship RCS models.

References

[1]   Alexander, J.; Loxodromes: A Rhumb Way to Go; *Mathematics Magazine*, Vol. 77, No. 5, pp 349-356, 2004.

[2]   Anastassopoulos, V.; G.A. Lampropoulos, A. Drosopoulos, and M. Rey; High Resolution Radar Clutter Statistics; *IEEE Transactions on Aerospace and Electronic Systems*, Vol. 35, No. 1, pp 43-60, 1999.

[3]   Lindgren, B.W.; Statistical Theory, 2nd ed.; MacMillan, Toronto, 1968.

[4]   Secker, J.; A Statistical Investigation into the Shape of the Globular Cluster Luminosity Distribution; *The Astronomical Journal*, Vol. 104, No. 4, pp 1472-1481, 1992.

[5]   Secker, J., P.W. Vachon, M. Robson, and J. Rowe; Assisted Acquisition Planning for Maritime Surveillance with Commercial Satellite Imagery; to appear, Proc. OceanSAR 2006 – The Third Workshop on Coastal and Marine Applications of SAR, St. John's, NL, Canada, October 2006.

[6]   Skolnik, M.; Radar Handbook, 2nd ed.; McGraw Hill, New York, 1990.

[7]   Tayebi, N., P.W. Vachon, J. Wolfe, and J. Secker (2006), Estimates of the CFAV *Quest* radar cross section from RADARSAT-1 SAR images: A comparison of results from several imagery exploitation tools, (DRDC Ottawa TN 2006-183) Defence R&D Canada – Ottawa. Internal publication.

[8]   Vachon, P.W., R.A. English, and J. Wolfe; Validation of RADARSAT-1 Vessel Signatures with AISLive Data; in press, *Canadian Journal of Remote Sensing*, 2007.

[9]   Vachon, P.W., J.W.M. Campbell, C. Bjerkelund, F.W. Dobson, and M.T. Rey; Ship detection by the RADARSAT SAR: Validation of detection model predictions; *Canadian Journal of Remote Sensing*, Vol. 23, No. 1, pp. 48-59, 1997.

[10]   Vachon, P.W., and J. Wolfe (2006), Modelling the Probability Density Function of Ship Radar Cross Section Measurements; Analysis of RADARSAT-1 Fine Mode and AISLive Data, (DRDC Ottawa TN 2006-271) Defence R&D Canada – Ottawa. Internal publication.

[11]   Vexcel Corp., EarthView SAR-APP, datasheet; (Online) http://www.vexcel.com/downloads/radar/datasheets/EV-SAR_APP.pdf (21 February 2007).

[12]   Williams, E. (2006); Aviation Formulary V1.43; (Online) http://williams.best.vwh.net/avform.htm (6 February 2007).

[13]   Wolfe, J.; VUSAR, A SAR Image Viewer; User Manual; Canada Centre for Remote Sensing technical report, Dec. 2002, 22 pages.

List of acronyms

A	Gamma or Log-Normal distribution shape parameter
AIS	Automatic Identification System
APP	EarthView Advanced Precision Processor
ATR	Automatic Target Recognition
B	Gamma or Log-Normal distribution scale parameter
CDF	Cumulative Distribution Function
CDPF	Canadian Data Processing Facility
CoG	Course over Ground
CSIAPS	Commercial Satellite Imagery Acquisition Planning System
DND	Department of National Defence
DR	Dead Reckoning
DRDC	Defence R&D Canada
GPS	Global Positioning System
IMO	International Maritime Organisation
ISR	Internet Ships Register
KSH	Kolomogorov-Smirnov Hypothesis
L	Ship Length
LH	Line Heading
LUT	look-up table
Mean	Sample Mean
MDA	MacDonald, Dettwiler and Associates Ltd.
MMSI	Maritime Mobile Service Identity
OMW	Ocean Monitoring Workstation
PDF	Probability Density Function
R-1	RADARSAT-1
R&D	Research & Development
RCS	Radar Cross Section
RSI	RADARSAT International
S5	Standard beam mode 5, RADARSAT-1
S6	Standard beam mode 6, RADARSAT-1
SAR	Synthetic Aperture Radar

SCNB	ScanSAR Narrow B (W2-S5-S6), RADARSAT-1
SoG	Speed over Ground
SPA	Swath Planning Application
STD	Sample Standard Deviation
UTC	Universal Coordinated Time
VHF	Very High Frequency
VUSAR	An xv-based SAR image analysis software
W2	Wide beam mode 2, RADARSAT-1
X1	Sample population #1
X2	Sample population #2

Distribution list

Document No.: DRDC Ottawa TM 2007-052

LIST PART 1: Internal Distribution by Centre:

4	Library DRDC Ottawa
1	Ryan English
1	Gary Geling
1	Chuck Livingstone
1	Jeff Secker
1	Paris Vachon
1	John Wolfe

10   TOTAL LIST PART 1

LIST PART 2: External Distribution by DRDKIM

1	CISTI
1	DRDKIM
3	Library and Archives Canada
1	LCol Jeff Howes, DPDOIS, Polar Epsilon
1	LCdr Robert Quinn, DJCP
1	LCdr Andy Samoluk, DJCP
1	Jake Tunaley, DPDOIS, Polar Epsilon
1	Caroline Wilcox, DSTC4ISR

10   TOTAL LIST PART 2

20   TOTAL COPIES REQUIRED

DOCUMENT CONTROL DATA
(Security classification of title, body of abstract and indexing annotation must be entered when the overall document is classified)

1. ORIGINATOR (The name and address of the organization preparing the document. Organizations for whom the document was prepared, e.g. Centre sponsoring a contractor's report, or tasking agency, are entered in section 8.) Defence R&D Canada - Ottawa 3701 Carling Avenue Ottawa, Ontario K1A 0Z4	2. SECURITY CLASSIFICATION (Overall security classification of the document including special warning terms if applicable.) UNCLASSIFIED

3. TITLE (The complete document title as indicated on the title page. Its classification should be indicated by the appropriate abbreviation (S, C, R or U) in parentheses after the title.)

Ship Signatures in RADARSAT-1 ScanSAR Narrow B Imagery: Analysis with AISLive Data

4. AUTHORS (last name, followed by initials – ranks, titles, etc. not to be used)

Vachon, P.W., English, R.A., Wolfe, J.

5. DATE OF PUBLICATION (Month and year of publication of document.) March 2007	6a. NO. OF PAGES (Total containing information, including Annexes, Appendices, etc.) 64	6b. NO. OF REFS (Total cited in document.) 13

7. DESCRIPTIVE NOTES (The category of the document, e.g. technical report, technical note or memorandum. If appropriate, enter the type of report, e.g. interim, progress, summary, annual or final. Give the inclusive dates when a specific reporting period is covered.)

Technical Memorandum

8. SPONSORING ACTIVITY (The name of the department project office or laboratory sponsoring the research and development – include address.)

Polar Epsilon SLA

9a. PROJECT OR GRANT NO. (If appropriate, the applicable research and development project or grant number under which the document was written. Please specify whether project or grant.) 15ec06-01, 15ec23	9b. CONTRACT NO. (If appropriate, the applicable number under which the document was written.)
10a. ORIGINATOR'S DOCUMENT NUMBER (The official document number by which the document is identified by the originating activity. This number must be unique to this document.) DRDC Ottawa TM 2007-052	10b. OTHER DOCUMENT NO(s). (Any other numbers which may be assigned this document either by the originator or by the sponsor.)

11. DOCUMENT AVAILABILITY (Any limitations on further dissemination of the document, other than those imposed by security classification.)

(X) Unlimited distribution
(   ) Defence departments and defence contractors; further distribution only as approved
(   ) Defence departments and Canadian defence contractors; further distribution only as approved
(   ) Government departments and agencies; further distribution only as approved
(   ) Defence departments; further distribution only as approved
(   ) Other (please specify):

12. DOCUMENT ANNOUNCEMENT (Any limitation to the bibliographic announcement of this document. This will normally correspond to the Document Availability (11). However, where further distribution (beyond the audience specified in (11) is possible, a wider announcement audience may be selected.))

13. ABSTRACT (A brief and factual summary of the document. It may also appear elsewhere in the body of the document itself. It is highly desirable that the abstract of classified documents be unclassified. Each paragraph of the abstract shall begin with an indication of the security classification of the information in the paragraph (unless the document itself is unclassified) represented as (S), (C), (R), or (U). It is not necessary to include here abstracts in both official languages unless the text is bilingual.)

RADARSAT-1 ScanSAR Narrow B (SCNB) mode imagery at 50 m (nominal) spatial resolution of high density shipping regions were acquired along with contemporaneous Automatic Identification System (AIS) data via an AISLive snapshot service. Within the images are 1805 signatures of isolated ships ranging from 40 m to 350 m in length, for which AIS data, including ship identification, size, and velocity, are available.

The AIS data were verified through an authoritative ship database, which identified errors in the static AIS data. Dynamic errors were also characterized since pairs of location observations were available. The mean error between the AIS-predicted ship position and the ship signature position (124 m) is smaller than the average ship length in the overall data set (147 m).

The data were used to model the radar cross section (RCS) of ships in SCNB data as a simple geometric function of the ship length. The variability about the normalized RCS, a consequence of ship type, local incidence angle, ship aspect angle, and sea state, could not be described by a single probability density function, but a Log-Normal distribution was appropriate for certain ship length ranges. Ship RCS variability observed in the SCNB data is consistent with that observed previously in Fine mode data, but there is an overall scaling differing between the SCNB and Fine mode data sets.

This work demonstrates that the fusion of RADARSAT image signatures of ships with AIS data is straightforward and provides unprecedented insight to observed ship signatures. However, the AIS data, at least the static fields, should be routinely verified prior to fusion with other sources of ship information.

14. KEYWORDS, DESCRIPTORS or IDENTIFIERS (Technically meaningful terms or short phrases that characterize a document and could be helpful in cataloguing the document. They should be selected so that no security classification is required. Identifiers, such as equipment model designation, trade name, military project code name, geographic location may also be included. If possible keywords should be selected from a published thesaurus, e.g. Thesaurus of Engineering and Scientific Terms (TEST) and that thesaurus identified. If it is not possible to select indexing terms which are Unclassified, the classification of each should be indicated as with the title.)

RADARSAT-1, SAR, synthetic aperture radar, ScanSAR, Automatic Identification System, AIS, AISLive

Defence R&D Canada

Canada's leader in Defence
and National Security
Science and Technology

R & D pour la défense Canada

Chef de file au Canada en matière
de science et de technologie pour
la défense et la sécurité nationale

DEFENCE R&D DÉFENSE

www.drdc-rddc.gc.ca